



Goddard Space Flight Center Greenbelt, MD



Rev- 001 Effective Date: 01/13/2025

Commercial Satellite Data Acquisition Program ICEYE U.S. Radiometric & Geometric Quality Assessment Report

Signature/Approval Page

Approval by:		
Melissa Yang Martin Commercial Satellite Data Acquisition Program Manager	Date	
Earth Science Division		
Headquarters/NASA		
Accepted by:		
Dana Ostrenga	Date	
Commercial Satellite Data Acquisition Project Manager		
Earth Science Division		
GSEC/NASA		

Rev- 001

Effective Date: 01/13/2025

Preface

This document is under CSDA Project configuration control. Once this document is approved, CSDA approved changes are handled in accordance with Class I and Class II change control requirements described in the CSDA Configuration Management Procedures based on NASA standard configuration practices, and changes to this document shall be made by document change notice (DCN), documented in the Change History Log or by complete revision.

Abstract

The evaluation summarized in this report was conducted by subject matter experts (SMEs) funded by NASA's Commercial Satellite Data Acquisition (CSDA) Program. The SMEs evaluated the radiometric and geometric quality of ICEYE U.S. data for the NASA Earth science research and applications community. The results of the evaluation help to inform NASA program management on the quality of the data for NASA science.

Cover Art: Cover art is AI generated graphic using Microsoft Copilot Designer using term "commercial satellite constellation Earth observation across Atlantic AND Northern Hemisphere AND digital downlink"

Authored and prepared by

Batuhan Osmanoglu

CSDA SAR Subject Matter Expert National Aeronautics and Space Administration

Jordan Bell

CSDA ICEYE Evaluation Team Lead National Aeronautics and Space Administration

Jaime Nickeson

CSDA Technical Science Coordinator Science Systems and Applications Inc National Aeronautics and Space Administration

MinJeong Jo

SAR Quality Assessment Expert University of Maryland, Baltimore County National Aeronautics and Space Administration

Dylan Boyd

SAR Evaluation Assistant University of Maryland, College Park National Aeronautics and Space Administration

Frederick Policelli

CSDA Project Scientist
National Aeronautics and Space Administration

Change History Log

Revision	Effective Date	Description of Changes
1.0	01/13/2025	First Draft Completed

Rev- 001 Effective Date: 01/13/2025

Table of Contents

\mathbf{E}	xecut	tive	Summary	. 9
1	C	al/V	al Maturity Matrices	11
	1.1	Sui	mmary Cal/Val Maturity Matrix	11
	1.2	De	tailed Validation Maturity Matrix	12
2	D	ata l	Provider Documentation Review	12
	2.1	Pro	oduct Information	12
	2.2	M	etrology	15
	2.3	Pro	duct Generation	16
3	D	etail	ed Validation – Radiometric	18
	3.1	Ab	solute Radiometric Calibration	18
	3.	1.1	Method	18
	3.	1.2 I	Results Compliance	19
	3.2	Rac	diometric Stability	20
	3.	2.1	Method	
	3.	2.2	Results Compliance	20
	3.3	Ser	nsitivity Validation	
	3	3.1	Method	
	3	3.2	Results Compliance	21
	3.4	Pol	arimetric Accuracy	
	3.	4.1	Method	22
	3.5	Inte	erferometric Accuracy	22
	3	5.1	Method	
		5.2	Results Compliance	
4	D	etail	ed Validation – Geometric	22
	4.1	Spa	atial Resolution	
	4.	1.1	Method	28
	4.	1.2	Results Compliance	28
	4.2	Ge	olocation Accuracy	
	4.	2.1	Method	
	4.	2.2	Results Compliance	35
5	\mathbf{R}	efer	ences	41

List of Figures

Figure 1. Summary Cal/Val Maturity Matrix for ICEYE U.S	11
Figure 2. Detailed Validation Maturity Matrix for the SAR domain	
Figure 3. Sigma ₀ values observed across a swath over various sites in the Amazon	
Figure 4. Noise Equivalent Sigma Zero (NESZ) as observed over the Doldrums	21
Figure 5. The upper image is a Google Earth overview of the location of the Rosamond CR	
Figure 6. A Google Earth view of the NISAR Calibration array in Oklahoma.	
Figure 7. The Neustrelitz, Germany CR site	27
Figure 8. The Sodankylä, Finland CR site	
Figure 9. The IRF of the Rosamond CR ID 08 in scene SM_950305792	31
Figure 10. The IRF of the Oklahoma N03K CR in scene SM_4103746	33
Figure 11. Demonstration of geolocation accuracy assessment.	35
Figure 12. Geolocation errors of all analyzed ICEYE images over Rosamond, CA	38
Figure 13. Geolocation errors of ICEYE SM and SL mode	38
List of Tables	
Table 1. Summarized list of ICEYE acquisitions used for the radiometric assessment	
Table 2. Absolute calibration and radiometric stability results over Rosamond, CA	
Table 3. The expected NESZ values of various ICEYE imaging modes	
Table 4. ICEYE interferometric stability over the 9 out of 12 2.4-m CRs over Rosamond	
Table 5. Summarized list of ICEYE acquisitions used for the IRF assessment.	
Table 6. Corner Reflectors used for the analysis at the Rosamond site.	
Table 7. Corner Reflectors used for the analysis at the Oklahoma site.	
Table 8. Corner Reflectors used for the analysis at the Neustrelitz site.	
Table 9. Corner Reflectors used for the analysis at the Sodankylä site.	
Table 10. The IRF quality values for the ICEYE products.	
Table 11. Observed spatial resolution, PSLR and ISLR at Rosamond, CA	
Table 12. Observed spatial resolution, PSLR and ISLR over Oklahoma CR site.	
Table 13. Observed spatial resolution, PSLR and ISLR over Neustrelitz, Germany	
Table 14. Observed spatial resolution, PSLR and ISLR over Sodankylä, Finland	
Table 15. Expected geolocation accuracies provided in the ICEYE SAR Product Guide	
Table 16. Rosamond geolocation accuracy analysis for ICEYE.	
Table 17. Geolocation accuracy analysis over the Oklahoma site	
Table 18. Geolocation accuracy analysis over the Neustrelitz site.	
Table 19. Geolocation accuracy analysis over the Sodankylä site	
Table A1. Detailed list of ICEYE acquisitions used for the radiometric assessment.	
Table A2. Detailed list of ICEYE acquisitions used for the IRF assessment.	45

Acronyms & Abbreviations

ALE	Absolute Location Error
CR	
CSDA	
DLR	
EDAP	Earthnet Data Assessment Pilot
ЕО	Earth Observation
ESA	European Space Agency
EULA	1 1 0 7
FAIR	Findable, Accessible, Interoperable, Reusable
FMI	Finnish Meteorological Institute
GeoTIFF	Geographic Tag Image File Format
GRD	Ground Range Detected
GSFC	Goddard Space Flight Center
GTR	
IGARSS	*
Н5	
IRF	Impulse Response Function
InSAR	Interferometric SAR
ISCE	InSAR Scientific Computing Environment
ISLR	Integrated Side-Lobe Ratio
ISRO	Indian Space Research Organization
JPL	Jet Propulsion Laboratory
JSON	
KML	Keyhole Markup Language
MERRA-2	Modern-Era Retrospective Analysis for Research and Applications,
	Version 2
N/A	11
NASA	1
NESZ	1 &
NISAR	NASA-ISRO SAR
PNG	Portable Network Graphic
PSLR	Peak Side-Lobe Ratio
RCRA	Rosamond Corner Reflector Array
RMSE	Root Mean Square Error
RPM	Rigorous Projection Model
SAR	Synthetic Aperture Radar
S3	Simple Storage Service (Amazon Cloud)
SC	Scan Mode / ScanSAR Mode
SFTP	Secure File Transfer Protocol
SL	Spot Mode / Spotlight Mode

Rev- 001

Effective Date: 01/13/2025

SLC	Single-Look Complex
SLEA	Spotlight Extended Area
SLH	Spot/Spotlight, High-Resolution
SM	Strip Mode / StripMap Mode
SMH	Strip/Stripmap Mode, High-resolution
SNAP	Sentinel Application Platform
StaMPS	Stanford Method for Persistent Scatterers
SVG	Scalable Vector Graphics
USG	United States Government
VV	Vertical-vertical (polarization)
WGS84	World Geodetic System 1984
XML	Extensible Markup Language

Rev- 001

Effective Date: 01/13/2025

Executive Summary

The Commercial Satellite Data Acquisition (CSDA) Program was established to identify, evaluate, and acquire data from commercial sources that support the National Aeronautics and Space Administration (NASA) Earth science research and application goals. NASA's Earth Science Division (ESD) recognizes the potential impact commercial satellite constellations may have in encouraging/enabling efficient approaches to advancing Earth System Science and applications development for societal benefit. Commercially acquired data may also provide a cost-effective means to augment and/or complement the suite of Earth observations acquired by NASA and other U.S. government agencies and those by international partners and agencies.

In this report, CSDA provides an evaluation of the quality of data provided by the ICEYE U.S. (referred hereafter as ICEYE) X-band Synthetic Aperture Radar (SAR) satellite constellation for advancing NASA's Earth system science research and applications. This evaluation of ICEYE radiometric and geometric performance was carried out by NASA subject matter experts (SMEs) that were enlisted to evaluate the fundamental quality of the ICEYE data following the Joint NASA/European Space Agency (ESA) assessment guidelines (ESA-NASA, 2024).

Data from the ICEYE constellation of satellites, identified as X2-X37, were analyzed, with satellite X7 providing daily coherent Ground Track Repeat (GTR) data. The data products provided by ICEYE included in this analysis were between product version 1.100 and 1.93. Details about an assessment performed by a group of selected principal investigators on the utility of ICEYE U.S. data for NASA science is available in a separate report, the *Commercial Satellite Data Acquisition Program ICEYE U.S. Principal Investigator Evaluation Summary*.

Only the documents provided by ICEYE for the evaluation were considered as part of the assessment. Additional documentation with more detailed description of the calibration and validation procedures may be available online, but any document that is not listed in this report were not considered for the evaluation. The product information provided in the vendor documentation guides and the product metadata together provide adequate information to work with the data. The product details in the metadata were provided in the common extensible markup language (XML) file format. These documents provide a characterization of the SAR system and data, together with the metadata, that also includes relevant ancillary information. Documentation provided to CSDA included limited pre- and post-flight calibration information. Metrological traceability was not included in documentation provided to CSDA.

The quality assessment was mainly performed on the single look complex (SLC) Level 1 data products, while Ground Range Detected (GRD) Level 2 data were used for Scan (SC) mode. Additional Level 2 products were used in the science usability evaluation report by the Principal Investigator team. The uncertainty values relevant for SAR (i.e. noise equivalent sigma zero [NESZ]) are not provided at the product level in the metadata. The NESZ instead is provided as a single value in the ICEYE Product Documentation. A "calibration factor" for each product is provided in the metadata to convert the observed radar brightness to meaningful units (i.e. sigma₀). Expected and observed values for relevant metrics, such as absolute radiometric accuracy, relative radiometric accuracy, NESZ, peak sidelobe ratio (PSLR), and integrated sidelobe ratio (ISLR) are

Rev- 001

Effective Date: 01/13/2025

discussed within the results compliance sections of this document. The vendor provided documentation does not contain information on how these performance values are obtained.

An independent quality assessment of the essential quality parameters of SAR, such as spatial resolution, PSLR, ISLR, NESZ, absolute and relative radiometric accuracy was performed by the SME team. Representative datasets collected by ICEYE over various test sites, including both distributed and point targets, were used. Note that the nomenclature used by ICEYE varies slightly from those commonly used. In this report, the use of Spot, refers to Spotlight mode along with the acronym SL, Spotlight High-resolution is abbreviated as SLH, Spotlight Extended Area is denoted as SLEA, Stripmap mode is referred to as simply Strip or SM, and ScanSAR mode is referred to as Scan, or as mentioned above, SC. Each of these collection modes from ICEYE were analyzed by CSDA. The validation by the CSDA Program was performed using multiple software packages, including code developed internally at NASA Goddard Space Flight Center (GSFC), the GAMMA Remote Sensing commercial processing package, ESA's Sentinel Application Platform (SNAP) architecture, and the Stanford Method for Persistent Scatterers (StaMPS) software. In addition to these software packages, the PI teams also processed the data using JPL's InSAR (interferometric SAR) Scientific Computing Environment (ISCE). The quality analysis results were generally in agreement with the values provided by ICEYE U.S., such as spatial resolution and geolocation accuracy. The measured PSLR values were generally close to the expected theoretical values. Based on the available ICEYE documentation and our independent data analysis, we conclude that the ICEYE U.S. data are of good quality.

1. Cal/Val Maturity Matrices

1.1 Summary Cal/Val Maturity Matrix

Data Provider Documentation Review			
Product Information	Metrology	Product Generation	
Product Details	Radiometric Calibration & Characterization	Radiometric Calibration Algorithm	
Availability & Accessibility	Geometric Calibration & Characterization	Geometric Processing	
Product Format, Flags & Metadata	Metrological Traceability Documentation	Retrieval Algorithm (if L0)	
User Documentation	Uncertainty Characterization	Mission Specific Processing	
	Ancillary Data		

Validation Summary
Radiometric Validation Method
Radiometric Validation Results Compliance
Geometric Validation Method
Geometric Validation Results Compliance



Figure 1. Summary Cal/Val Maturity Matrix for ICEYE U.S.

Rev- 001 Effective Date: 01/13/2025

1.2 Detailed Validation Maturity Matrix

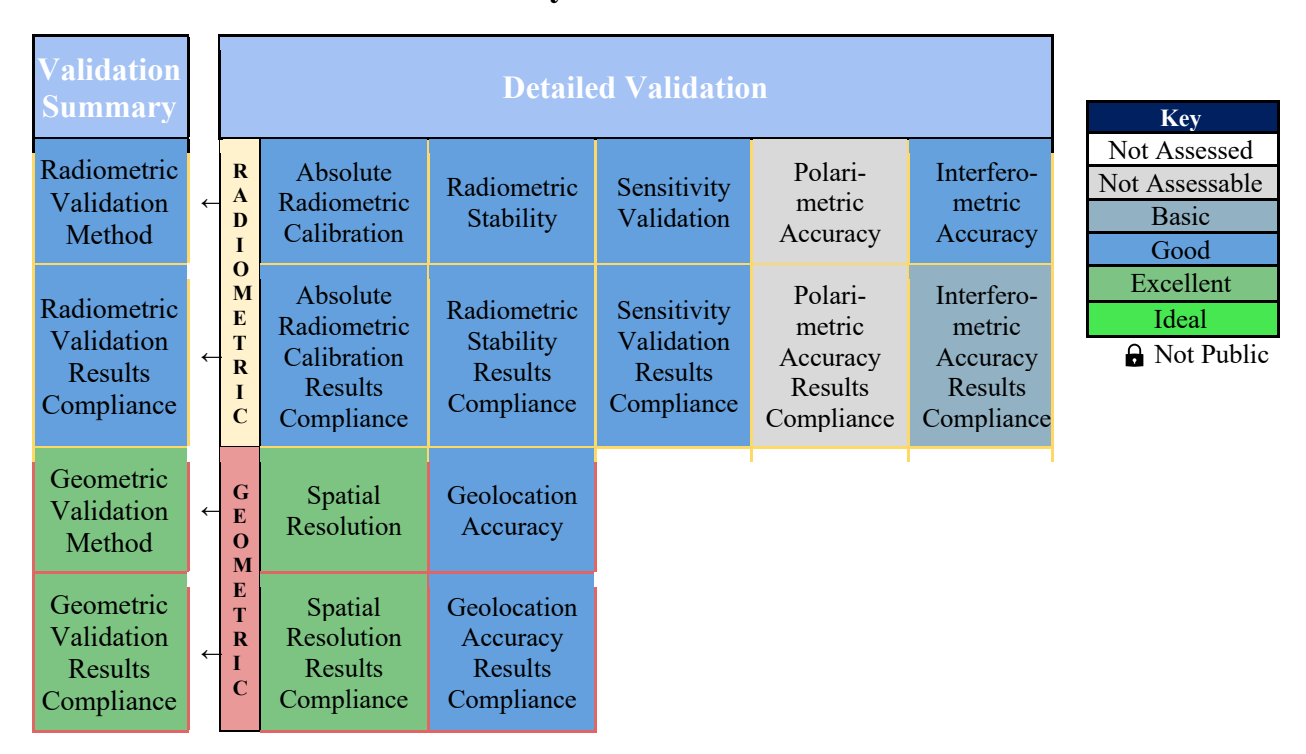


Figure 2. Detailed Validation Maturity Matrix for the SAR domain, showing the Validation Summary column from the Summary Cal/Val Maturity Matrix.

2. Data Provider Documentation Review

2.1 Product Information

Product Details			
Grade: Excellent			
Justification	Product details are well defined in reference documentation and supporting metadata.		
Product Name	ICEYE_XN_PPL_Mode_IIIII_yyyymmddThhmmss.ext Where: • XN – Satellite ID • PPL – Product processing level • Mode – Imaging mode (SL, SLH, SM, SMH, SC) • IIIII – Product ID • yyyymmddThhmmss acquisition start date/time • ext – extension, file format (h5, json, png, tif, xml, kml)		
Sensor Name	ICEYE X-band Radar Satellites		

Rev- 001 Effective Date: 01/13/2025

Sensor Type	SAR			
Mission Type	Constellation – 13 satellites at the beginning of evaluation.			
Mission Orbit	Sun-synchronous			
Product Version Number	1.100 to 1.93			
Product ID	A number within the Product Name with four to five digits unique for each product.			
Processing level of product	Level 1 (SLC and GRD products)			
Measured Quantity Name	GRD Products	ghtness β_0 , (IC) and radar cross so		Product Guide)
Measured Quantity Units	Radar brightness β_0 and normalized radar cross section σ_0 are unitless quantities representing reflectivity per unit area.			
Stated Measurement Quality	Noise and Geospatial Errors Noise-equivalent Geospatial		6	
Spatial Resolution	For SLC Spot Strip For GRD Spot Scan Strip	Azimuth [m] 0.25 3 Azimuth [m] 1 < 15 3	Slant Ran 0.5 0.5 to Ground R 1.5 to	2.5 ange [m] 0 0.9 15
Spatial Coverage	Spot Spot Extended Scan Strip	Range [k 5 15 100 30		nuth [km] 5 15 100 50
Temporal Resolution	The ICEYE documentation assures that areas of interest can achieve 24-hour repeat pass. The first ICEYE satellite, X1, was launched January 12, 2018.			
Temporal Coverage	·		and had 7 satellites	

	imagery used in this evaluation spans from October 2019 to April 2024.
Point of Contact	Joselyne Hernandez-Romero, joselyne.romero@iceye.us Garry Engle, garry.engle@iceye.us Allegra Scott, allegra.scott@iceye.us
Product locator (DOI/URL)	N/A
Conditions for access and use	All data used in this evaluation were purchased by CSDA under U.S. Government-wide license. Licenses can be found on the CSDA website (https://www.earthdata.nasa.gov/about/csda/commercial-datasets).
Limitations on public access	N/A
Product Abstract	N/A

Availability & Accessibility		
Grade: Good		
Justification	Meets 15/17 of FAIR guiding principles. Unfulfilled principles are A2: Metadata are accessible, even when the data are no longer available I3: (Meta)data include qualified references to other (meta)data	
Compliant with FAIR principles	88%	
Data Management Plan	The vendor data management plan is described in • ICEYE Product Documentation v5.0	
Availability Status	Archive imagery is commercially available to users with a vendor-provided account.	

Product Format, Flags & Metadata				
Grade: Good				
Justification Image datasets are provided in png, tif, and h5 formats v supporting metadata found in h5 and xml files. For a convenience, h5 and xml metadata are largely redundant. Level 1 imagery and metadata are organized by nested fold indicating year, month, day, and product ID.				
Product File Format	tif, xml, kml, h5 and png			
Metadata Conventions Metadata v2.4, indicated by the spec_version xml tag.				
Analysis Ready Data?	No			

User Documentation				
Grade: Good				
Justification The user documentation and associated references provided to CSDA evaluators detail many aspects of product generation and the required auxiliary data. However, the documents do not provide traceable quality information for the provided uncertainty values.				
Document	Reference	QA4ECV Compliant		
Product User Guide and Information	ICEYE SAR Product Guide (ICEYE, 2022c) (Accessed: March 20, 2023)	No		
	ICEYE Level 1 Product Format Specification Document (ICEYE, 2020)	No		
	ICEYE SAR Mission Brochure (ICEYE, 2022b)	No		
	ICEYE SAR Data Brochure (ICEYE, 2022a).	No		
ATBD	Not available. Some details in the documentation files above.			

2.2 Metrology

Radiometric Calibration & Characterization				
Grade: Basic				
Justification Relevant SAR characterization is described. Pre- and post-flip SAR calibration is minimal in the provided documentation is absent from associated metadata.				
References	 ICEYE SAR Product Guide (ICEYE, 2022c) ICEYE Level 1 Product Format Specification Document (ICEYE, 2020) 			

Geometric Calibration & Characterization				
Grade: Basic				
Justification	Geometric calibration is described in the ICEYE Product Documentation, with a worst-case RMSE of 6 m, over calibration sites. Areas without corner reflectors are expected to have increased errors according to documentation. Data and methods used by the vendor to determine this geometric calibration error were not available to the evaluation team.			
References	ICEYE SAR Product Guide (ICEYE, 2022c)			

Metrological Traceability Documentation				
Grade: Not Assessable				
Justification	The evaluation team did not have access to metrological traceability documentation.			
References	N/A			

Uncertainty Characterization				
Grade: Basic				
Justification	Many relevant parameters are provided in the metadata, but methods for reproducing these metrics are not described.			
References	• ICEYE Level 1 Product Format Specification Document (ICEYE, 2020)			

Ancillary Data				
Grade: Good				
Justification	Ancillary data used in product generation are specified, although not necessarily on a per product basis, in the product metadata (e.g. DEM field does not state which DEM was used or that a DEM was used). Mostly of a sufficient quality to be judged "fit for purpose" in terms of mission's stated performance.			
References	• ICEYE Level 1 Product Format Specification Document (ICEYE, 2020)			

2.3 Product Generation

Radiometric Calibration Algorithm					
Grade: Good					
Justification SAR image generation is described in the ICEYE documes below. Calibration coefficients are provided in the metada Description of radiometric calibration methods are limited terms of reproducibility in the context of science applications the provided documentation.					
References	 ICEYE SAR Product Guide (ICEYE, 2022c) ICEYE Level 1 Product Format Specification Document (ICEYE, 2020) 				

Geometric Processing					
Grade: Excellent					
Justification	The geometric processing of SAR imagery is detailed in the ICEYE Level 1 Product Format Specification Document, with further references therein. Ground-projected SAR imagery is generated by a Rigorous Projection Model (RPM) wherein pixels are projected over a World Geodetic System 1984 (WGS84) ellipsoid. Supporting equations are provided in documentation, and the parameters for RPM are provided in metadata alongside ground-range-to-slant-range data. Geometric processing is reproducible and well documented.				
References	 ICEYE SAR Product Guide (ICEYE, 2022c) ICEYE Level 1 Product Format Specification Document (ICEYE, 2020) 				

Retrieval Algorithm				
Grade: Not Assessable				
Justification	Higher-level data products are beyond the scope of this study. The primary service of this commercial constellation is ondemand SAR imagery with configurable resolution and scene extent. A dedicated higher-level data product is not currently associated with this constellation.			
References	N/A			

Mission Specific Processing				
Grade: Not Assessable				
Justification	This assessment is restricted to the provided SLC and ground-projected SAR data products. No additional evaluation of mission specific data products such as classification maps or deformation maps are performed in this evaluation.			
References	N/A			

Rev- 001

Effective Date: 01/13/2025

3. Detailed Validation – Radiometric

This section presents the detailed measurement validation such as the absolute radiometric accuracy, radiometric stability, sensitivity and interferometric assessments conducted with ICEYE US dataset. For the radiometric analyses, the sigma₀ was calculated according to the ICEYE SAR Product Guide (ICEYE, 2022c):

$$\sigma_{0dB} = 10 \log 10 \left(CF |DN_{SLC}|^2 \sin(\theta) \right)$$

where CF denotes calibration factor, DN_{SLC} is the dynamic number in the SLC product and θ is the incidence angle. This analysis includes data from the ICEYE constellation that are shown in Table 1.

Table 1. Summarized list of ICEYE acquisitions used for the radiometric assessment. A detailed list of the parameters for individual satellite scenes used in the assessment is available in Appendix A, Table A1.

Test Area	Satellite Number	Imaging Mode	Number of Scenes	Acquisition Date	Incidence Angle	Processor Version
Rosamond, CA	Various	SM	8	02/22/2020 - 08/16/2021	28.4 - 33.7	1.916
	X7	SM (GTR)	31	05/10/2022 - 09/05/2022	36.1 - 37.1	1.94
	Various	SM	6	05/30/2024 - 06/04/2024	14.0 - 32.7	1.1, 1.916
Doldrums	Various	SLH	11	01/20/2023 - 06/30/2024	23.6 - 39.3	1.1, 1.101, 1.916
	Various	SLEA	7	04/07/2023 - 04/08/2023	20.9 - 29.0	1.1
Amazon	Various	SM	10	05/30/2024 - 06/18/2024	15.8 - 33.3	1.1, 1.916
	Various	SLH	20	05/29/2021 - 07/01/2024	20.8 - 34.3	1.1, 1.101, 1.916
	Various	SLEA	4	06/01/2024 - 07/02/2024	20.5 - 35.1	1.101, 1.917
	X11, X35	SC	2	7/1/24	23.2 - 23.6	1.101

3.1 Absolute Radiometric Calibration

3.1.1 Method

The absolute radiometric accuracy of the imagery was validated using scenes over the Amazon rainforest and the Rosamond corner reflector array (RCRA). The Amazon rainforest was used as a distributed target under the assumption that it represents a uniform and invariant target across the swath. It is also assumed that the uncertainty in measurement of the sigma₀ is zero (i.e., speckle is ignored). For a point target, such as the corner reflectors at Rosamond, the absolute radiometric accuracy measures the uncertainty in measurement of the radar cross section (RCS) considering an invariant and well-known ground target.

3.1.2 Results Compliance

The expected sigma₀ value over a tree covered surface at X-band VV-polarization for incidence angles between 13.5 and 35.8 degrees is about -9.8 dB (Ulaby et al., 2019). The calibrated ICEYE sigma₀ values have a mean value of -4.5 dB, or within about 4.3 dB of our expectation, with the SC scene ID 4141133 showing the lowest value and the SM scene ID 950305346 showing the highest value.

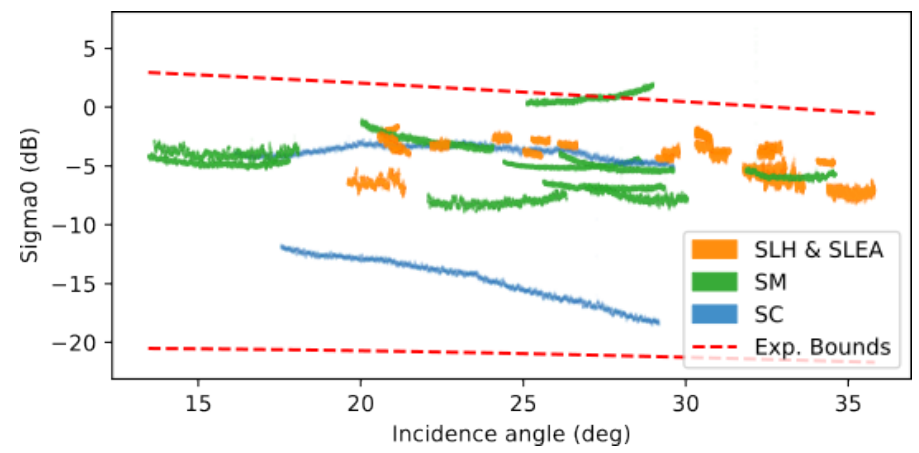


Figure 3. Sigma₀ values observed across a swath Amazon sites indicate that most of the scenes fall within the expected range. The dashed red lines mark +/- 3-sigma values for the expected range of X-band VV sigma₀ values, per (Ulaby et al., 2019).

The RCRA has 0.7-m, 2.4-m and 4.8-m corner reflectors. A set of 8 ascending, left-looking, VV-polarization images from X2, X4, X7 and X9 satellites were analyzed. The 0.7-m corner reflectors are most suitable for the high-resolution X-band sensors and have a mean absolute error of 0.3 dB. The 2.4-m and 4.8-m reflectors are better suited for L- and P-band sensors and show mean absolute errors of -21.2 and -19.4 dB respectively (Table 2).

Table 2. Absolute calibration and radiometric stability results over Rosamond, CA corner reflector test site.

		Observed (dB)		Error (dB)	
CR ID	Size (m)	Mean	Std	Mean	Std
28	0.7	10.6	5.2	-17.5	5.3
31	0.7	20.6	7.3	-5.4	6.8
33	0.7	36.2	13.2	12.6	12.7
34	0.7	21.0	7.2	-0.8	6.4
13	2.4384	35.9	3.5	-13.8	3.5
14	2.4384	22.4	6.4	-27.8	6.1
15	2.4384	25.8	11.6	-24.7	11.3
16	2.4384	26.8	11.9	-23.9	11.8
17	2.3989	34.2	11.4	-15.7	11.2
18	2.4384	23.8	13.0	-26.7	12.8
19	2.4384	30.3	12.5	-19.5	12.2
23	4.8	37.6	13.4	-19.1	12.7
24	4.8	35.3	12.8	-21.5	12.0
25	4.8	36.6	13.0	-20.1	12.4
26	4.8	43.9	3.6	-13.1	3.2
27	4.8	35.0	12.0	-21.7	11.1

Rev- 001

Effective Date: 01/13/2025

3.2 Radiometric Stability

3.2.1 Method

Radiometric stability of the imagery was validated using the Amazon rainforest and the Rosamond site. The Amazon rainforest was used as a distributed target under the assumption that it represents a uniform and invariant target across the swath and assuming that the temporal variation of the target area is minimal. The corner reflectors at the Rosamond site were used as stable, well-defined targets. Radiometric stability was then calculated based on the repeated independent measurements of the reflectivity (sigma₀) of a stable target. This target can be situated anywhere within the system dynamic range and swath assuming that the uncertainty in measurement of the sigma₀ is zero (i.e., speckle is ignored).

3.2.2 Results Compliance

The expected variation of sigma₀ value over a tree covered surface at X-band VV-polarization for incidence angles between 13.5° and 35.8° is about 3.7 dB (Ulaby et al., 2019). As shown in Figure 3, the calibrated ICEYE sigma₀ values have an overall standard deviation of 2.5 dB.

Over the Rosamond site, there are 3 corner reflector sizes, and the subset that was used for the stability analysis is shown in Table 2. The 0.7 m corner reflectors have a temporal variability of about 5.2-13.2 dB, while the 2.4 m and the 4.8 m corner reflectors have a temporal variability of 3.5-13.0 and 3.6-13.4 dB, respectively.

Although a few corner reflectors at the Rosamond site exhibited radiometric stability greater than 10 dB, the stability observed over the Amazon rainforest was reasonable and rated as good. Therefore, the overall radiometric stability performance of the ICEYE imagery was assessed as good.

3.3 Sensitivity Validation

3.3.1 Method

NESZ is estimated using signal-free regions (e.g., over very low or null backscatter targets, such as calm water or deserts) in the radar imagery. For this analysis, we used imagery over the Doldrums. Near surface level (2 m above ellipsoid) wind conditions at the time of each acquisition were also observed through the closest surface-level wind estimate of the Modern-Era Retrospective Analysis for Research and Applications, Version 2 (MERRA-2) reanalysis (Gelaro et al., 2017) to ensure that the observations were on typically calm days (wind speed < 2 m/s). The expected sigma₀ values were calculated using a geophysical model function. The XMOD2 (Li & Lehner, 2013) model was used for this analysis.

3.3.2 Results Compliance

The ICEYE NESZ was assessed by collecting imagery over the Doldrums using Spot, Strip and Scan imagery. ICEYE defines the expected NESZ for these products in the ICEYE SAR Product Guide (ICEYE, 2022c), shown in Table 3.

Table 3. The expected NESZ values of various ICEYE imaging modes per vendor documentation.

	Spot & Spot Extended Area	Strip	Scan
NESZ (dBm²/m²)	-18 to -15	-21.5 to -20	-22.2 to -21.5
Performant Incidence Range (deg)	20 to 35	15 to 30	21 to 29

Figure 4 shows the observed sigma₀ values over various ICEYE images at varying angles. The received backscatter is a function of the sensor's incidence angle. It must be noted that the maximum performant incidence angle for ICEYE is limited to 35 degrees, leaving a valid analysis range of about 7-8 degrees between ~27 and 35 degrees. This is mainly because the incidence angle reduces the expected sigma₀ lower than the published NESZ values.

In Figure 4, we see that near the valid incidence angle range, the ICEYE observed sigma₀ values over the Doldrums are on average 2-3 dB above the solid red line indicating good NESZ performance, which was calculated with the assumption of a 2 m/s wind speed. This analysis estimates the expected backscatter using the XMOD2 model and is bounded with wind speeds estimated close to the time of acquisition using MERRA-2 (Gelaro et al., 2017) data, excluding any scene that was collected with wind speeds above 4 m/s. The average wind speed for the scenes included in the analysis were 3.0 m/s with a standard deviation of 0.8 m/s. We note the recommended validity range for incidence angles using XMOD2 extends from 20 to 45° (Li & Lehner, 2013).

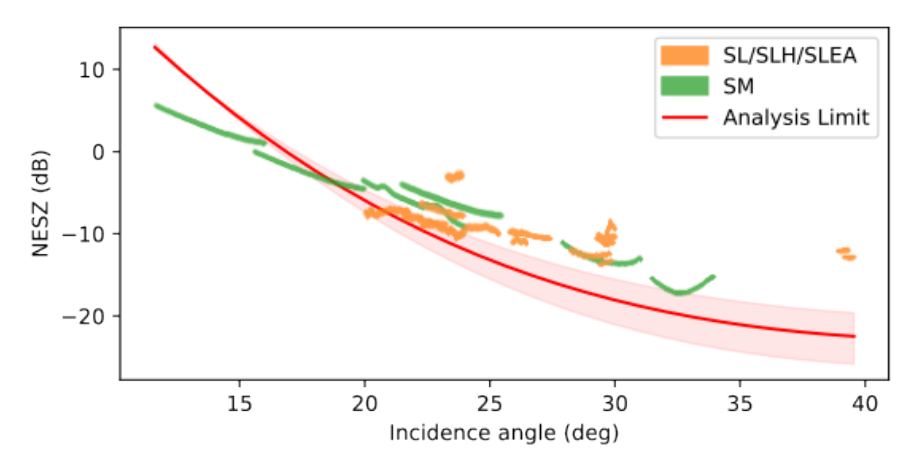


Figure 4. Noise Equivalent Sigma Zero (NESZ) as observed over the Doldrums. The solid red line indicates the XMOD2 calculated sigma $_0$ for a 2 m/s wind speed at ICEYE center frequency of 9.65 GHz. The red shaded area indicates expected analysis limits. The scatter plots show the observed sigma $_0$ across the swath.

3.4 Polarimetric Accuracy

3.4.1 Method

Polarization accuracy can be measured using corner reflectors if quad polarization imagery is available (van Zyl, 1990). ICEYE imagery was limited to VV polarization acquisitions at the time of this evaluation. Therefore, polarimetric accuracy was not validated.

3.5 Interferometric Accuracy

3.5.1 Method

The interferometric quality is assessed through tracking of point target phase over time for various targets across the image swath (Marinkovic et al., 2007). The analysis was conducted using interferometric acquisitions over the Rosamond site. Interferograms were formed through standard interferometric processing chains within SNAP and GAMMA software, and time series coherence analysis was conducted through StaMPS software (Hooper, 2007).

3.5.2 Results Compliance

While the expected coherence at the location of a corner reflector can be as high as 0.98 in a well-calibrated and stable CR installation, the average coherence reached over the corner reflectors with a stack of 23 single reference co-registered images is around 0.5. Even though the initial stack had 31 scenes, 8 scenes (20220525, 20220526, 20220527, 20220601, 20220609, 20220611, 20220810, 20220827) were removed due to co-registration failure. After the co-registration, of the 12 potential 2.4-m corner reflectors only nine of them display coherence values over 0.4.

Table 4. ICEYE interferometric stability over the 9	out of 12 2.4 m corner reflectors at the Rosamond, CA site.
-----------------------------------------------------	-------------------------------------------------------------

CR_ID	Size (m)	Lon	Lat	Observed Coherence	Expected Coherence
3	2.4384	-118.0819	34.8053	0.49	0.98
4	2.4384	-118.0764	34.8054	0.70	0.98
5	2.4384	-118.0708	34.8055	0.54	0.98
6	2.4384	-118.0652	34.8056	0.54	0.98
7	2.4384	-118.0595	34.8057	0.52	0.98
8	2.4384	-118.0540	34.8058	0.56	0.98
9	2.4384	-118.0489	34.8058	0.65	0.98
11	2.4384	-118.0377	34.8060	0.45	0.98
12	2.4384	-118.0323	34.8061	0.44	0.98

4. Detailed Validation – Geometric

This section describes detailed information of the Impulse Response Function (IRF) quality assessment using point target analysis tools provided in the GAMMA software package. The test datasets are collected from various ICEYE satellites from X2 to X37, including Strip (SM), Spot

(SL), and Spot High-resolution (SLH) mode scenes in SLC format. In addition, four Scan (SC) mode scenes formatted as GRD products were analyzed over four different calibration sites. Table 5 lists the ICEYE data products used for the IRF quality assessment, showing test areas, satellite ID numbers, imaging modes, scene ID numbers, acquisition dates, incidence angles, and processor versions of the products provided by the vendor.

The IRF analysis was performed over dedicated calibration sites with trihedral corner reflectors (CRs). The calibration sites used in this study include the Rosamond Corner Reflector Array (RCRA) in Rosamond, CA, the NASA/Indian Space Research Organization SAR (NISAR) Oklahoma Calibration Array found in multiple cities across Oklahoma, the German Aerospace Center (DLR) Neustrelitz calibration site in northern Germany, and the Finnish Meteorological Institute (FMI) calibration site in Sodankylä, Finland. For the Rosamond site, 29 SM scenes, 53 SL/SLH scenes, and 4 SC scenes were analyzed. For the Oklahoma site, 19 SM scenes and 7 SLH scenes were analyzed. Additionally, 11 SLH scenes and 6 SL/SLH scenes were analyzed for the Neustrelitz and Sodankylä sites, respectively. Table 5 shows the summarized list of ICEYE images used for the IRF analysis. Detailed information on each scene can be found in the list in Appendix A, Table A2.

Table 5. Summarized list of ICEYE acquisitions used for the IRF assessment. A detailed list of the parameters for individual satellite scenes used in the assessment is available in Appendix A, Table A2.

Test Area	Satellite Number	Imaging Mode	Number o	of Scene	S	Acquisition Date	Incidence Angle	Processor Version
	Various	SM	29		1/31/2020 - 07/11/2024	16.4963 - 35.0269	1.101, 1.916	
Rosamond	Various	SL/SLH	53			07/11/2020 - 06/05/2024	20.7382 - 37.2182	1.1, 1.916
	X12, X13	SC	4			05/16/2023	21.4994 - 29.5819	1.916
Oklahoma	Various	SM	19		05/29/2024 - 06/15/2024	15.7514 - 34.6509	1.1	
	Vario	ous	SLH	7	05/29/2024 - 06/15/2024	23.9228 - 37.8026	1.	.1
Neustrelitz	X11 - 2	X13	SLH 11		01/26/2023 - 03/05/2023	21.8082 - 33.3238	1.	.1
Sodankylä	X4		SL/SLH	6	08/23/2020 - 11/02/2020	21.3028 - 27.476	1.	.1

The Rosamond array is located near the south shore of the Rosamond dry lakebed in the desert of southern California (Fig. 5). The array consists of 38 triangular trihedral CRs in 3 sizes and oriented east or west, as depicted in Figure 5. Five 4.8-meter and five 0.7-m CRs are oriented mostly eastward with an azimuth heading of 350°. The remaining five 0.7-m CRs have a heading angle of 90°. Of the twenty-three 2.4-m CRs, ten face mostly east, while the remaining thirteen are oriented west with an azimuth heading of 170°. Table 6 lists all of the CRs installed at the Rosamond site. The coordinates of the CRs were retrieved for December 13, 2023.



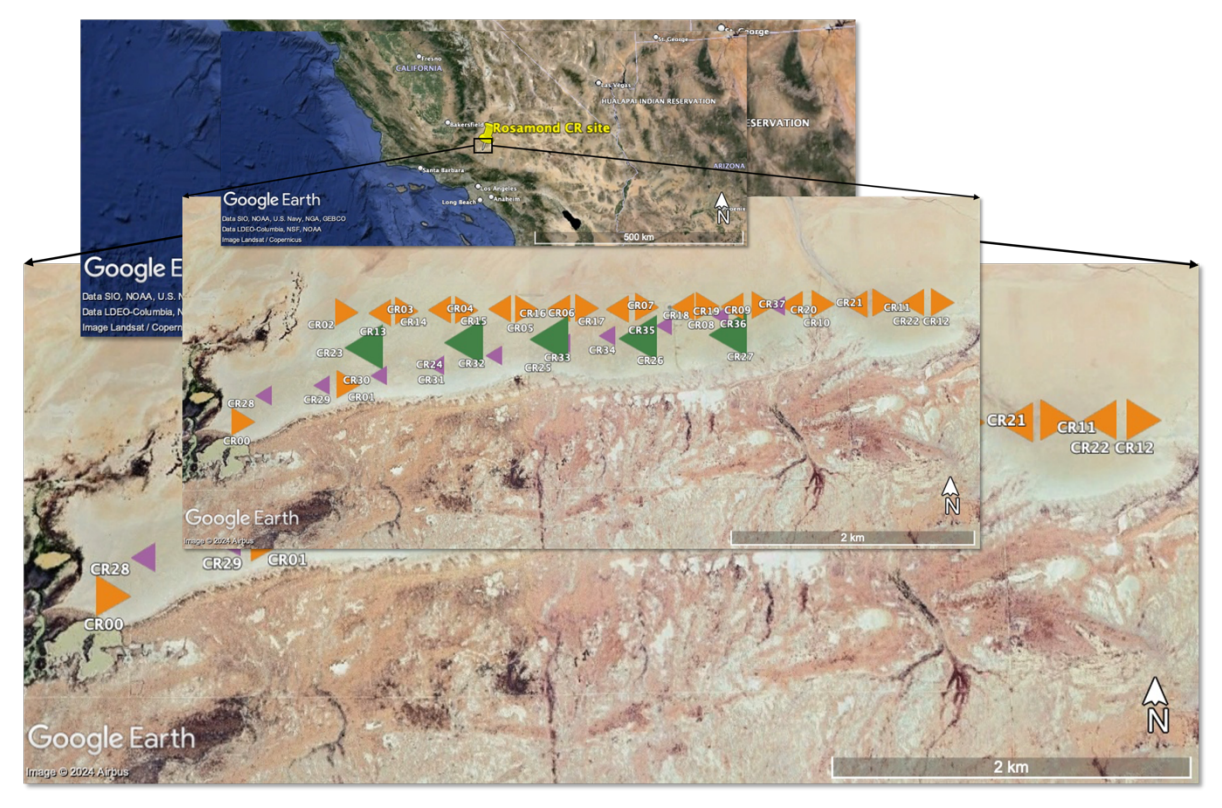


Figure 5. The upper image is a Google Earth overview of the location of the Rosamond CR array site in the Southern California desert. The lower image shows a closer view of the CR site, showing the CR names, alignment, and orientation.

Table 6. Corner Reflectors used for the analysis at the Rosamond site (Data collected 2023-12-13).

CR ID	Latitude (°)	Longitude (°)	Height Above Ellipsoid (m)	Orientation (°)	Elevation angle (°)	Size (m)
0	34.79696928	-118.0965308	660.7856	170.5	12.1	2.4384
1	34.79984853	-118.0869888	661.0345	170.5	8.72	2.4384
2	34.80523754	-118.0873892	660.7958	170	9.3	2.4384
3	34.80533834	-118.0819448	660.9918	170	8.63	2.4384
4	34.80541548	-118.0763782	661.1546	176	11.93	2.4384
5	34.8054937	-118.0708033	661.2243	171	11.07	2.4384
6	34.80558476	-118.0652258	661.2514	170	10.53	2.4384
7	34.80566746	-118.0596983	661.4008	170	14.7	2.4384
8	34.80575785	-118.0540222	661.5722	170.25	14.53	2.3989
9	34.80581413	-118.0489155	661.4449	175	10.63	2.4384
10	34.80592451	-118.043414	661.5768	170	14.6	2.4384
11	34.80602484	-118.0377366	661.7009	170	14.6	2.3989
12	34.80607395	-118.0323022	661.9127	169.5	8.1	2.4384
13	34.80519273	-118.0844198	660.9361	347	11.9	2.4384
14	34.80544015	-118.0789224	661.1566	350	16	2.4384
15	34.80552371	-118.0732806	661.3502	350.5	14.2	2.3989

16	34.80554864	-118.0678693	661.2834	350	8.03	2.4384
17	34.80555364	-118.0626289	661.3211	346	11	2.4384
18	34.80568769	-118.0564284	661.4424	346	8.97	2.4384
19	34.80572728	-118.0517598	661.5665	351.25	13.8	2.3989
20	34.80583804	-118.0463581	661.4455	350	10.77	2.4384
21	34.80590043	-118.0403334	661.4684	352	8.67	2.4384
22	34.80605059	-118.0351916	661.8013	9.8	16	2.4384
23	34.80250457	-118.0858055	661.1996	351.06	21	4.8
24	34.80290959	-118.0766468	661.4277	350.97	20.9	4.8
25	34.8031567	-118.0687806	661.5126	349.69	21	4.8
26	34.80322846	-118.0605826	661.6268	350.66	20.82	4.8
27	34.80351967	-118.0522806	661.646	349.64	20.93	4.8
28	34.79888379	-118.0948328	661.7686	9.9	15.05	0.8
29	34.79972489	-118.0895138	661.6029	91.5	34	0.7
30	34.80045797	-118.0843113	661.7026	91	33.8	0.7
31	34.80122329	-118.0790953	661.9545	351	16.7	0.7
32	34.80198195	-118.0737944	661.8988	90.5	33.2	0.7
33	34.80291898	-118.0675155	661.9962	354	20	0.7
34	34.80349615	-118.0633929	662.0635	354	21.9	0.7
35	34.80426739	-118.0581255	662.1272	91	31.6	0.7
36	34.80501201	-118.0528936	662.0533	92	31.5	0.7
37	34.80577951	-118.0476745	662.2021	351	28.1	0.7

The Oklahoma NISAR Calibration Array is grouped into clustered sites in the northern (Enid), western (Clinton), and southern (Lawton) regions of Oklahoma (Fig. 6). Since June 2021, seventeen (17) 2.8-m triangular trihedral CRs have been deployed. Table 7 lists the CRs installed at the Oklahoma sites. Nineteen SM scenes and 7 SLH scenes were acquired over the Oklahoma CR sites. Because the Enid, Clinton, and Lawton corner reflector array sites are separated by distances of several hundred kilometers, each scene covers different CR sites. Although N02K and N04K, as well as N01K and N03K, are co-located, N01K and N04K were not visible due to their differing facing directions and were therefore excluded from this analysis.

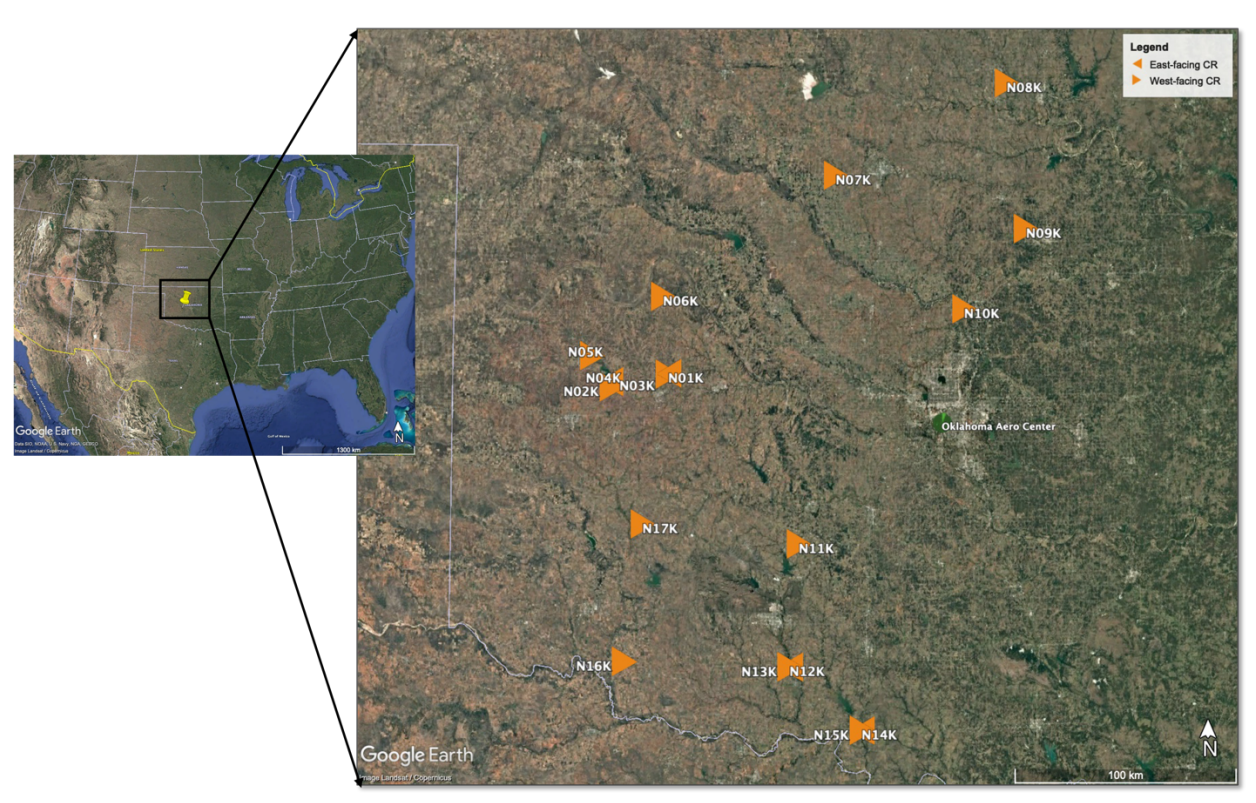


Figure 6. A Google Earth view of the NISAR Calibration array in Oklahoma. The triangles show CR names and distribution at the site.

Table 7. Corner Reflectors used for the analysis at the Oklahoma site (Data collected 2024-05-01).

CR ID	Latitude (°)	Longitude (°)	Height Above Ellipsoid (m)	Orientation (°)	Elevation angle (°)	Size (m)
N02K	35.53645899	-99.21004135	481.1742	179.76	17.17	2.8
N03K	35.58880383	-98.93568414	479.2929	180.95	14.9	2.8
N05K	35.66009168	-99.3084363	479.2629	182.01	14.7	2.8
N06K	35.89871953	-98.96084099	561.1503	181.96	16.6	2.8
N07K	36.38462466	-98.11048857	368.6874	178.99	14.37	2.8
N08K	36.7549092	-97.2545799	272.6516	179.86	17.33	2.8
N09K	36.16779644	-97.16946796	267.8307	176.27	15.73	2.8
N10K	35.84867938	-97.48050174	300.9426	177.03	15.43	2.8
N11K	34.91477489	-98.29206887	413.9211	180.46	15.4	2.8
N12K	34.42325112	-98.33622533	284.0768	180.85	16.93	2.8

Figure 7 shows the DLR's Neustrelitz calibration site in Northern Germany. This site contains four permanently installed trihedral CRs with a face width of 1.5-meters. Corner reflectors D33, D35, and D36 face west and D34 faces east. As shown in Figure 7, only the three CRs facing west are detected in the ICEYE scene. These CRs at the DLR site are primarily used for long-term

monitoring of the Airbus TerraSAR-X, TanDEM-X and PAZ satellites. The coordinates and elevation of the Neustrelitz site were obtained from ESA's Earthnet Data Assessment Pilot (EDAP) Technical Note on quality assessment of ICEYE (Ruiz & Cohen, 2024), however information about the CR orientation was not available. Table 8 lists details of the DLR CRs installed at the Neustrelitz site.

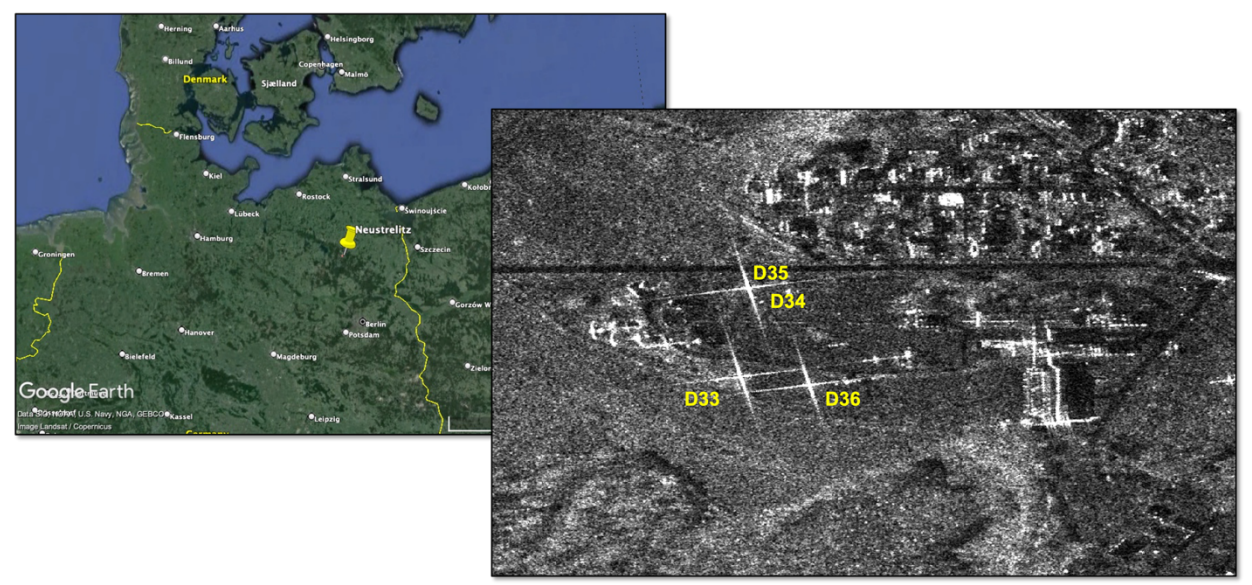


Figure 7. The Neustrelitz, Germany site (https://calvalportal.ceos.org/neustrelitz-germany - accessed 09/2024) marked on Google Earth (left). The CRs observed by the ICEYE SL satellite image (right).

Table 8. Corner Reflectors used for the analysis at the Neustrelitz site (Date collected is unknown).

CR ID	Latitude (°)	Longitude (°)	Height Above Ellipsoid (m)	Size (m)
D33	53.32945	13.06939	106	1.5
D34	53.33008	13.06963	109	1.5
D35	53.33020	13.06952	109	1.5
D36	53.32938	13.06991	104	1.5

Figure 8 shows the Sodankylä airfield site located in northern Finland managed by FMI. In 2020, four CRs were installed within the Sodankylä airfield, all of which are oriented west, with an azimuth angle of 241.83° which represents the boresight angle of the CR. This value can represent an azimuth heading angle of 151.83° using the simple conversion factor of

$$\varphi_{azimuth} = \varphi_{heading} + 90^{\circ}$$
.

Additionally, the incidence angle of 24.83° was converted into the elevation angle of 65.17° (Table 9).

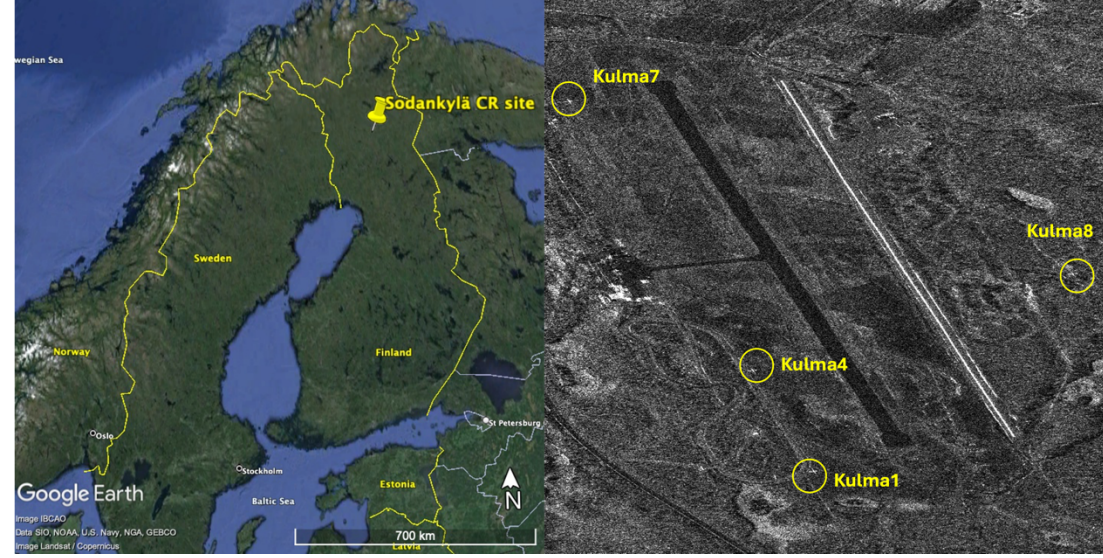


Figure 8. The Sodankylä, Finland CR site marked on Google Earth (left). The CRs in Sodankylä site observed by the ICEYE satellite (right). The bright point targets show the CRs on the SAR image.

Table 9. Corner Reflectors used for	r the analysis at the Sodankylä	site (Data collected: 2020-09-01).

CR ID	Latitude (°)	Longitude (°)	Height Above Ellipsoid (m)	Orientation (°)	Elevation angle (°)	Size (m)
kulma8	26.629641	67.394678	183.51	151.83	65.17	0.9
kulma7	26.611566	67.400821	181.59	151.83	65.17	0.9
kulma4	26.618219	67.391239	181.79	151.83	65.17	0.9
kulma1	26.620403	67.387648	181.40	151.83	65.17	0.9

4.1 **Spatial Resolution**

4.1.1 Method

The spatial resolution of the imagery was validated using point target analysis tools provided in the GAMMA software, such as the SLC version of the point target analysis command ptarg SLC, which estimates the 3 dB peak widths in range and azimuth for a given corner reflector. The expected slant range and azimuth resolutions are provided in the product metadata files. Assessment of the spatial resolution for ICEYE imagery was performed using four different corner reflector calibration sites, a) Rosamond, CA, b) Oklahoma, c) Neustrelitz, Germany, and d) Sodankylä, Finland.

4.1.2 Results Compliance

Table 10 shows the quality metrics related to the spatial resolution and radar IRF provided in the ICEYE SAR Product Guide (ICEYE, 2022c). The documentation provides spatial slant range and azimuth resolution for the SM, SLH, and SLEA products. However, radar IRF metrics are not

provided for the Scan mode product since no SLC images are available for Scan mode data. ICEYE indicates a ground resolution of 15 m for the Scan mode product.

Table 10. The IRF quality values for the ICEYE products, provided in the ICEYE documentation.

Image Mode	Range Resolution [m]	Azimuth Resolution [m]	PSLR [dB]	ISLR [dB]
SM	0.5 to 2.5	3		
SL/SLH	0.5	0.25	-13.2	-5.03
SLEA	0.5	1.0		
SC	Ground resolution 15 m		N	A

The IRF quality parameters, PSLR and ISLR, for ICEYE satellites are not provided in public documentation. Instead, the reference values for PSLR and ISLR were gathered from the IGARSS conference paper that ICEYE published in 2020 (Ignatenko et al., 2020). In their previous analysis, ICEYE defined -13.2 dB for PSLR and -5.03 dB for ISLR.

Table 11, Table 12, Table 13, and Table 14 show the observed spatial resolution, PSLR, and ISLR of each image of the evaluation sites.

4.1.2.1 Rosamond, CA, USA

For the Rosamond site, we analyzed 29 Strip, 53 Spot, and 4 Scan mode images to calculate spatial resolution in range and azimuth directions. Table 11 lists the results of the IRF analysis for the various ICEYE satellites over the Rosamond site. The table includes the average and the standard deviation of all detected CRs of the scenes.

Table 11. Observed spatial resolution, PSLR and ISLR values in azimuth and range directions over Rosamond, CA.

Sat. #	Img Mode	Scene ID	Rg Resolution [m]	Az Resolution [m]	Rg PSLR [dB]	Az PSLR [dB]	Rg ISLR [dB]	Az ISLR [dB]
X2	SM	22728	1.16 ± 0.07	2.74±0.11	-13.75±0.35	-14.02±0.22	-12.85±0.17	-12.50±0.15
X4	SM	24338	1.08 ± 0.07	2.67±0.10	-12.76±0.28	-14.42±0.20	-11.44±0.14	-12.84±0.14
X4	SM	29630	1.00 ± 0.05	2.74 ± 0.10	-13.10±0.22	-14.19±0.31	-11.45±0.17	-12.70±0.28
X4	SM	33818	1.16 ± 0.08	2.74 ± 0.12	-12.95±0.28	-14.07±0.81	-11.46±0.23	-12.46±0.81
X7	SM	38803	1.03 ± 0.06	2.74±0.11	-12.97±0.28	-14.12±0.48	-11.44±0.17	-12.69±0.42
X7	SM	41079	1.19 ± 0.07	2.81±0.10	-13.05±0.28	-14.45±0.17	-11.48±0.17	-12.94±0.20
X2	SM	49376	0.98 ± 0.08	2.76 ± 0.09	-12.90±0.38	-14.03±0.32	-11.56±0.32	-12.45±0.29
X9	SM	105173	1.03 ± 0.07	2.78 ± 0.08	-13.06±0.36	-14.30±0.49	-11.53±0.43	-12.62±0.58
X37	SM	950309957	0.99 ± 0.08	2.76 ± 0.13	-12.41±0.60	-14.02±1.05	-11.30±0.74	-12.49±1.18
X36	SM	950310040	0.89 ± 0.05	2.77±0.12	-12.63±0.67	-14.27±0.53	-11.27±0.59	-12.71±0.49
X14	SM	950310385	0.73 ± 0.05	2.76 ± 0.09	-12.55±1.12	-14.15±0.59	-11.14±0.92	-12.66±0.56
X34	SM	950310614	0.94 ± 0.06	2.78 ± 0.11	-12.64±0.40	-14.26±1.05	-11.27±0.25	-12.89±0.50
X4	SM	20064	1.32 ± 0.08	2.67 ± 0.09	-19.38±0.98	-14.23±0.71	-19.06±1.21	-12.88±0.49
X5	SM	21756	1.06 ± 0.08	2.70 ± 0.09	-13.14±0.40	-13.81±0.39	-11.65±0.27	-12.44±0.43
X2	SM	23758	0.99 ± 0.08	2.71±0.08	-13.06±0.35	-13.98±0.20	-11.67±0.35	-12.45±0.20
X2	SM	33603	0.91 ± 0.05	2.71±0.12	-12.78±0.73	-13.65±0.75	-11.36±0.52	-12.10±0.72
X2	SM	35082	0.94 ± 0.07	2.71±0.11	-12.88±0.42	-13.72±0.29	-11.43±0.35	-12.38±0.25

	Img		Da Desolution	Az Pasalution				
Sat. #	Mode							Az ISLR [dB]
X7	SM	39010	1.04 ± 0.07	2.74 ± 0.11	-13.01±0.39	-14.41±0.35	-11.42±0.48	-12.82±0.33
X2	SM	39920	0.94 ± 0.07	2.73 ± 0.10	-13.01±0.37	-13.72±0.72	-11.55±0.21	-12.31±0.47
X2	SM	52027	0.94 ± 0.08	2.83±0.10	-12.90±0.70	-13.16±0.55	-11.39±0.41	-11.35±0.37
X12	SM	1877717	0.92 ± 0.06	2.79 ± 0.12	-13.11±0.57	-13.60±1.02	-11.45±0.59	-12.34±1.21
X27	SM	950304863	1.09 ± 0.06	2.78 ± 0.09	-13.08±0.35	-14.43±0.36	-11.27±0.27	-12.91±0.21
X14	SM	950305095	1.21±0.08	2.77 ± 0.07	-12.99±0.87	-14.12±0.76	-11.33±0.81	-12.57±0.90
X27		950305577	1.06 ± 0.07	2.74 ± 0.10	-13.15±0.21	-14.36±0.34	-11.33±0.26	-12.91±0.15
X30	SM	950305792	1.22 ± 0.08	2.78 ± 0.09	-10.40±1.01	-14.29±0.62	-10.05±0.92	-12.76±0.49
X37	SM	950309860	0.79 ± 0.04	2.75 ± 0.10	-12.32±1.02	-13.56±1.43	-11.00±0.81	-12.08±1.34
X36	SM	950309942	0.95 ± 0.06	2.77±0.10	-12.54±1.37	-13.72±1.10	-10.97±1.11	-12.30±1.12
X34	SM	950310092	0.54 ± 0.03	2.74 ± 0.13	-12.40±0.97	-13.67±1.78	-10.83±1.05	-12.15±1.54
X30		950310551	0.78 ± 0.26	2.76 ± 0.12	-12.17±0.83	-13.45±1.57	-10.33±0.88	-12.31±1.19
X4	SL	34834	0.46 ± 0.03	0.22 ± 0.02	-13.28±0.07	-12.87±0.34	-11.69±0.04	-11.48±0.12
X2	SL	35167	0.47 ± 0.03	0.22 ± 0.01	-13.77±0.37	-12.75±0.54	-12.14±0.15	-11.46±0.19
X4	SL	35640	0.46 ± 0.03	0.22 ± 0.01	-13.32±0.13	-12.69±0.91	-11.70±0.13	-11.25±0.75
X4	SL	35534	0.45 ± 0.03	0.22 ± 0.01	-13.30±0.10	-12.13±0.87	-11.69±0.08	-11.14±0.46
X4	SL	36421	0.45 ± 0.03	0.22 ± 0.01	-13.30±0.13	-12.84±0.32	-11.69±0.07	-11.41±0.29
X4	SL	37413	0.45 ± 0.02	0.22 ± 0.02	-13.30±0.10	-12.14±1.46	-11.68±0.11	-10.62±1.41
X4	SL	37414	0.47 ± 0.03	0.22 ± 0.01	-13.30±0.08	-12.77±0.19	-11.67±0.06	-11.25±0.13
X4	SL	38511	0.44 ± 0.03	0.22 ± 0.01	-13.33±0.06	-12.91±0.28	-11.69±0.06	-11.46±0.24
X4	SL	38600	0.44 ± 0.03	0.21 ± 0.01	-13.28±0.14	-12.83±0.32	-11.65±0.09	-11.50±0.24
X7	SL	38885	0.46 ± 0.02	0.22 ± 0.01	-13.53±0.14	-11.38±0.70	-11.84±0.08	-9.47±0.59
X4	SL	40398	0.44 ± 0.03	0.22 ± 0.01	-13.33±0.10	-12.61±0.87	-11.69±0.06	-11.34±0.49
X4	SL	40525	0.45 ± 0.04	0.21±0.01	-13.26±0.10	-12.78±0.26	-11.66±0.06	-11.40±0.15
X7	SL	40791	0.46±0.03	0.22±0.01	-13.52±0.18	-12.72±0.21	-11.77±0.12	-11.43±0.19
X2	SL	40975	0.45±0.03	0.21±0.01	-13.77±0.31	-12.78±0.30	-12.07±0.16	-11.38±0.21
X7	SL	41078	0.45±0.04	0.22±0.01	-13.47±0.28	-11.09±0.46	-11.78±0.17	-10.67±0.37
X13	SL	1690623	0.46±0.03	0.22±0.01	-13.07±0.84	-12.46±0.51	-11.56±0.86	-11.25±0.50
X2	SL	1690628	0.46±0.03	0.22±0.01	-13.22±0.27	-12.63±0.71	-12.22±0.54	-11.40±0.25
X13	SLH	4018201	0.46±0.03	0.21±0.01	-13.13±0.65	-12.78±1.01	-11.75±0.63	-11.27±0.85
X7	SLH	4020349	0.45±0.04	0.22±0.01	-13.27±0.40	-12.85±0.57	-11.49±0.13	-11.42±0.66
X8	SLH	4023256	0.47 ± 0.03	0.22±0.01	-13.69±0.72	-13.12±1.04	-12.18±0.67	-11.48±0.86
X13	SLH	4024972	0.45 ± 0.03	0.22±0.01	-13.52±0.31	-12.83±0.69	-12.02±0.31	-11.32±0.61
X7	SLH	4039742	0.46 ± 0.04	0.21±0.01	-13.15±0.65	-12.40±1.29	-11.31±0.73	-10.89±1.21
X4	SL	32885	0.43 ± 0.03	0.22±0.03	-13.22±0.56		-11.61±0.33	
X4	SL	35590	0.45 ± 0.03	0.21 ± 0.01	-13.35 ± 0.18	-13.01 ± 0.46	-11.73±0.10	-11.65 ± 0.40
X4 X2	SL SL	35591 36301	0.44 ± 0.02 0.45 ± 0.03	0.22±0.02 0.21±0.01	-13.27±0.29 -13.92±0.12	-13.12±0.65 -13.04±0.50	-11.67±0.15 -12.16±0.06	-11.49±0.44 -11.62±0.39
X4	SL							
X2	SL	37327 37833	0.44±0.02 0.46±0.04	0.21±0.01 0.22±0.01	-13.36±0.09 -13.59±0.85	-12.74±0.34 -12.83±0.76	-11.70±0.05 -11.99±0.48	-11.46±0.22 -11.66±0.26
X4	SL	38509		0.22±0.01 0.21±0.01				-11.00±0.20
X4 X4	SL	38510	0.45 ± 0.02 0.45 ± 0.03	0.21 ± 0.01 0.22 ± 0.01	-12.96±0.77 -13.38±0.06	-12.67±0.65 -12.97±0.16	-11.30±0.84 -11.68±0.08	-11.05 ± 1.10 -11.46 ± 0.19
X7	SL	39009	0.45 ± 0.03 0.46 ± 0.03	0.22 ± 0.01 0.22 ± 0.01	-13.84±0.09	-12.97 ± 0.16 -11.02 ± 0.14	-12.08±0.08	-10.90 ± 0.19
X7	SL	39009	0.40 ± 0.03 0.44 ± 0.03	0.22 ± 0.01 0.22 ± 0.01	-13.66±0.09	-9.75 ± 0.50	-12.08±0.10	-10.90±0.23
X4	SL	39484	0.44 ± 0.03 0.44 ± 0.03	0.22 ± 0.01 0.22 ± 0.01	-13.12±0.59	-9.73±0.30 -12.68±0.85	-11.87 ± 0.34 -11.53 ± 0.57	-10.01±0.44
X4	SL	40318	0.44 ± 0.03 0.44 ± 0.03	0.22 ± 0.01 0.22 ± 0.01	-13.12±0.39	-12.42±1.05	-11.58±0.37	-10.86±1.10
X4	SL	40393	0.44 ± 0.03 0.45 ± 0.04	0.22 ± 0.01 0.22 ± 0.01	-13.28±0.24	-12.42±1.03	-11.70±0.09	-10.86±1.10
X2	SL	40793	0.44 ± 0.03	0.21±0.01	-13.83±0.10	-12.94±0.37	-12.16±0.12	-11.53±0.33
X11	SL	1812330	0.46 ± 0.03	0.24 ± 0.02	-13.63±0.10	-13.57±1.12	-12.10±0.12	-12.54±1.22
X11	SL	1836121	0.46 ± 0.03	0.24 ± 0.02 0.23 ± 0.02	-12.97±1.20	-12.49 ± 0.55	-12.09±0.97	-11.61±0.72
X2 X2	SL	1839909	0.46 ± 0.03	0.23 ± 0.02 0.23 ± 0.02	-12.97±1.20	-13.42±1.07	-12.18±0.54	-12.46 ± 0.77
114	υL	1037707	U.TU±U.U3	0.4340.04	-12.7/40.00	-1J.7 <u>/</u> _1.0/	-12.10-0.34	-14.TU±U.//

Sat. #	Img Mode	Scene ID	Rg Resolution [m]	Az Resolution [m]	Rg PSLR [dB]	Az PSLR [dB]	Rg ISLR [dB]	Az ISLR [dB]
X30	SLH	950305104	0.48 ± 0.07	0.22 ± 0.02	-12.28±1.92	-12.15±1.10	-10.48±1.17	-10.87±1.00
X37	SLH	950305590	0.47 ± 0.05	0.22 ± 0.01	-11.92±1.19	-12.40±0.92	-10.32±1.04	-11.23±0.87
X36	SLH	950305803	0.48 ± 0.04	0.22 ± 0.02	-12.31±1.81	-11.90±0.76	-10.44±1.00	-10.73±1.05
X12	SL	1614898	0.45 ± 0.03	0.24 ± 0.01	-13.19±0.44	-15.00±1.06	-11.78±0.33	-13.89±0.75
X8	SL	1636472	0.47 ± 0.03	0.24 ± 0.02	-13.48±0.42	-13.82±0.66	-11.99±0.39	-12.56±0.61
X13	SLH	1821032	0.46 ± 0.03	0.22 ± 0.01	-13.58±0.37	-12.58±0.68	-11.92±0.26	-11.18±0.48
X8	SL	1833902	0.46 ± 0.03	0.24 ± 0.03	-13.64±0.84	-14.77±1.88	-11.89±0.47	-13.96±2.10
X13	SLH	1835028	0.45 ± 0.03	0.22 ± 0.01	-13.47±0.40	-12.54±0.55	-11.95±0.27	-11.16±0.47
X11	SL	1703151	0.46 ± 0.03	0.22 ± 0.01	-13.30±0.46	-12.94±0.55	-11.77±0.32	-11.34±0.50
X11	SL	1790820	0.44 ± 0.03	0.29 ± 0.03	-12.95±0.77	-17.17±1.44	-11.71±0.72	-16.85±1.37
X8	SL	1827332	0.44 ± 0.03	0.24 ± 0.06	-13.51±0.41	-13.35±0.67	-11.92±0.62	-12.50±0.84
X13	SLH	1835025	0.46 ± 0.03	0.22 ± 0.01	-13.41±0.61	-12.97±0.35	-11.84±0.74	-11.38±0.34
X12	SLH	1883416	0.45 ± 0.03	0.22 ± 0.02	-13.55±0.69	-12.72±1.08	-11.92±0.37	-11.29±1.12
X2	SL	2211313	0.46 ± 0.03	0.22 ± 0.01	-12.83±0.92	-12.83±1.00	-11.88±0.92	-11.17±0.89
X12	SC	2165262	2.09 ± 0.32	9.95±0.85	-22.84±5.49	-35.70±11.51	-23.02±5.17	-36.43±11.06
X12	SC	2227690	2.80±0.22	10.08±0.90	-22.04±4.30	-40.14±11.51	-22.46±4.14	-40.89±10.00
X12	SC	2165261	2.89±0.38	9.36±0.55	-20.69±5.31	-36.20±10.28	-21.50±5.41	-37.01±8.91
X13	SC	2184970	1.89±0.25	9.92±0.75	-23.26±7.66	-27.26±12.80	-25.01±7.19	-29.67±11.30

We also determined that the IRF of the Rosamond corner reflector, ID 08, in the SM image from ICEYE X30 satellite (scene ID 950305792), showed a double peak in the range direction (Fig. 9), which resulted in unreasonable PSLR and ISLR values from this corner reflector.

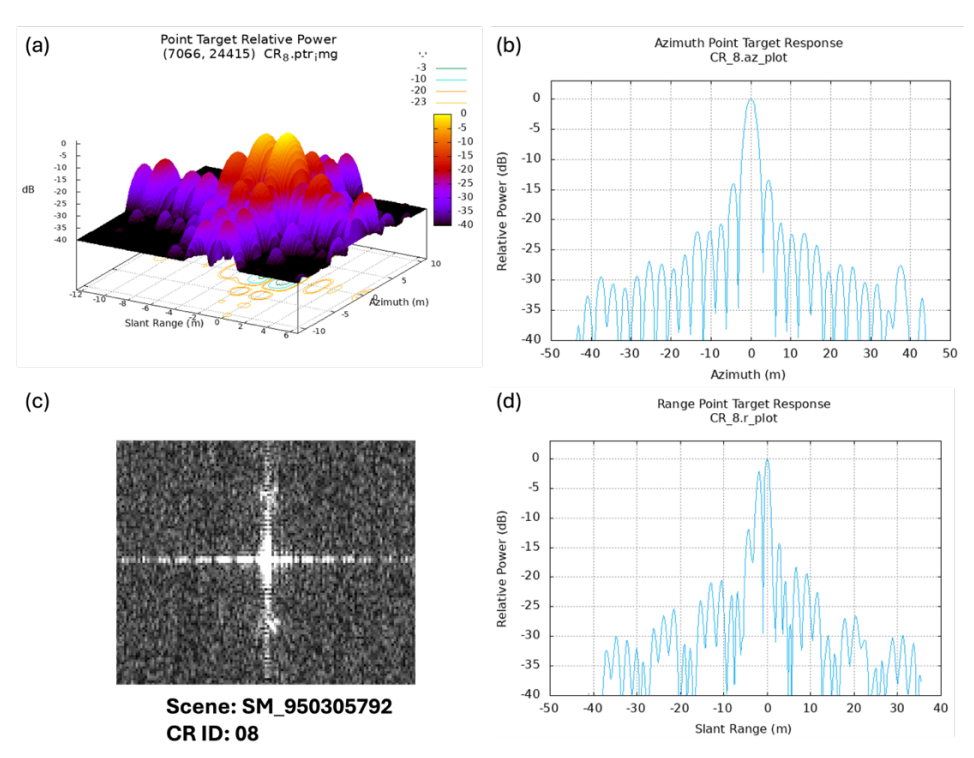


Figure 9. The IRF of the Rosamond CR ID 08 in scene SM_950305792. (a) 3D plot of CR relative power; (b) azimuth point target response plot; (c) the CR image in SLC; (d) range point target response plot.

4.1.2.2 Oklahoma, USA

For the Oklahoma site, we analyzed 19 Strip mode and 7 Spot mode images to calculate spatial resolution in the range and azimuth directions. Table 12 presents the results of the IRF analysis for various ICEYE satellites over the Oklahoma site. Each scene covers different CR locations, as the corner reflectors are separated by distances of tens of kilometers.

Table 12. Observed spatial resolution, PSLR and ISLR values in azimuth and range directions over Oklahoma.

Sat. #	Img Mode	Scene ID	Rg Resolution [m]	Az Resolution [m]	Rg PSLR [dB]	Az PSLR [dB]	Rg ISLR [dB]	Az ISLR [dB]
X13	SM	4104068	0.57	2.60	-12.55	-14.67	-11.07	-12.98
X13	SM	4108639	1.13	2.81	-12.91	-14.70	-11.42	-13.00
X13	SM	4113689	1.12	2.88	-13.01	-14.60	-11.60	-13.00
X19	SM	4118395	0.86	2.86	-13.23	-14.83	-12.88	-12.99
X19	SM	4122012	0.93	2.59	-13.78	-13.34	-12.29	-12.28
X20	SM	4103994	0.50	2.66	-13.15	-14.60	-11.80	-13.24
X20	SM	4113672	0.79	2.84	-12.90	-14.56	-11.40	-12.89
X23	SM	4103993	0.76	2.73	-12.82	-14.62	-11.38	-13.06
X31	SM	4102835	0.63	2.66	-12.59	-14.62	-11.21	-13.17
X31	SM	4109765	0.95	2.78	-12.78	-14.54	-11.53	-13.14
X31	SM	4118393	0.93	2.90	-12.54	-14.06	-11.45	-12.65
X35	SM	4108453	1.11	2.57	-12.81	-14.14	-11.26	-12.53
X35	SM	4109693	0.65	2.75	-13.71	-14.67	-11.71	-13.13
X35	SM	4117243	0.89	2.74	-13.29	-14.28	-11.63	-12.73
X7	SM	4107354	0.89	2.58	-13.42	-14.21	-11.68	-12.68
X7	SM	4108135	1.11	2.62	-13.25	-14.65	-11.46	-13.03
X8	SM	4107633	1.06	2.67	-13.38	-14.93	-11.63	-13.21
X8	SM	4122981	0.54	2.83	-13.50	-14.34	-11.75	-12.88
X11	SLH	4103169	0.42	0.22	-13.17	-13.13	-11.79	-11.33
X11	SLH	4108812	0.49	0.22	-13.15	-12.98	-11.70	-11.38
X20	SLH	4109826	0.42	0.23	-12.10	-13.10	-10.56	-11.49
X11	SLH	4113700	0.44	0.20	-13.20	-10.42	-11.79	-10.36
X11	SLH	4120049	0.44	0.21	-13.23	-11.61	-11.78	-11.20
X13	SLH	4123574	0.45	0.24	-13.35	-12.01	-11.88	-11.27
X7	SLH	4122664	0.48	0.23	-13.17	-13.18	-11.56	-11.39

In addition to the scenes listed in Table 12, we found that the SM image from the ICEYE X8 satellite, scene ID 4103746, at the Oklahoma site displayed double peak returns from the N03K corner reflector and did not allow for reliable measurements (Fig. 10).

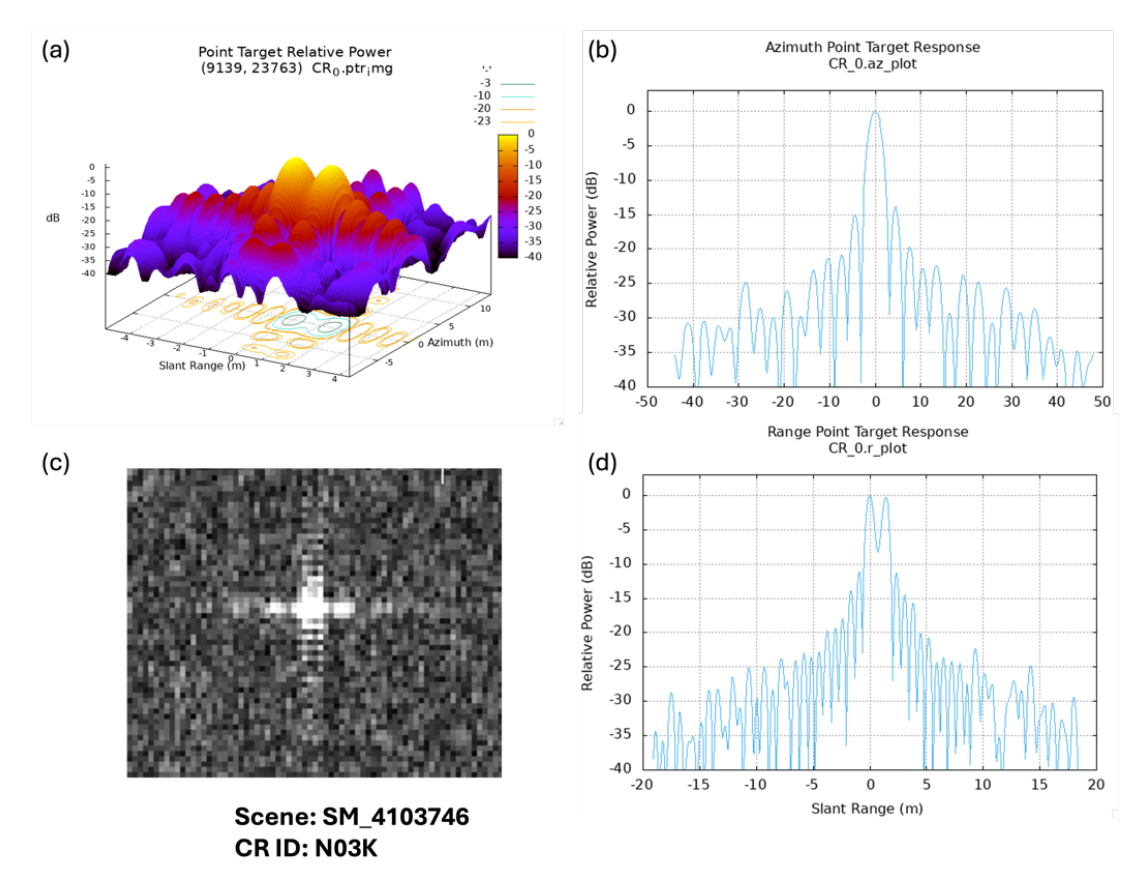


Figure 10. The IRF of the Oklahoma N03K CR in scene SM_4103746. (a) 3D plot of CR relative power; (b) azimuth point target response plot; (c) the CR image in SLC; (d) range point target response plot.

4.1.2.3 Neustrelitz, Germany

For the Neustrelitz site, we analyzed 11 Spot mode images to calculate spatial resolution in both the range and azimuth directions. Table 13 presents the results of the IRF analysis for the ICEYE X11–X13 satellites over the Neustrelitz site, including the average and standard deviation of three CRs detected in the scenes.

Table 13. Observed spatial resolution, PSLR and ISLR values in azimuth and range directions over Neustrelitz, Germany.

Sat. #	Img Mode	Scene ID	Rg Resolution [m]	Az Resolution [m]	Rg PSLR [dB]	Az PSLR [dB]	Rg ISLR [dB]	Az ISLR [dB]
X13	SLH	1821028	0.48 ± 0.02	0.22 ± 0.01	-13.52±0.06	-13.09±0.05	-11.97±0.00	-11.53±0.02
X11	SLH	1821033	0.41 ± 0.00	0.21 ± 0.01	-13.37±0.07	-13.07±0.04	-11.86±0.04	-11.49±0.06
X12	SLH	1839364	0.43 ± 0.02	0.21 ± 0.01	-13.84±0.06	-13.14±0.04	-12.12±0.05	-11.51±0.02
X13	SLH	1835026	0.46 ± 0.03	0.21 ± 0.01	-13.56±0.05	-13.09±0.18	-11.95±0.02	-11.49±0.09
X11	SLH	1881654	0.43 ± 0.01	0.21 ± 0.01	-13.20±0.01	-13.09±0.10	-11.79±0.03	-11.53±0.02
X13	SLH	1876905	0.44 ± 0.02	0.21 ± 0.01	-13.53±0.07	-12.72±0.23	-12.03±0.05	-11.49±0.04
X11	SLH	1872603	0.48 ± 0.01	0.22 ± 0.01	-13.16±0.05	-12.84±0.05	-11.75±0.01	-11.49±0.04
X12	SLH	1898700	0.46 ± 0.04	0.22 ± 0.02	-13.84±0.08	-12.88±0.14	-12.12±0.03	-11.47±0.02
X12	SLH	1923872	0.46 ± 0.03	0.22 ± 0.00	-13.73±0.02	-12.91±0.18	-12.06±0.03	-11.51±0.06
X12	SLH	1928906	0.45 ± 0.03	0.22 ± 0.00	-13.78±0.05	-12.64±0.07	-12.09±0.01	-11.52±0.01

In addition to the scenes listed in Table 13, we also found an anomalous issue with a single Spot acquisition from X12 (scene ID 1883417) that did not appear properly focused. Therefore, the spatial resolution and side lobes could not be calculated for this image.

4.1.2.4 Sodankylä, Finland

For the Sodankylä site, we analyzed six Spot mode images to calculate spatial resolution in both the range and azimuth directions. Table 14 presents the results of the IRF analysis for the ICEYE X4 satellite over the Sodankylä site, including the average and standard deviation of four CRs in the scenes.

 $Table~14.~Observed~spatial~resolution,~PSLR~and~ISLR~values~in~azimuth~and~range~directions~over~Sodankyl\"{a},~Finland.$

Sat. #	Img Mode	Scene ID	Rg Resolution [m]	Az Resolution [m]	Rg PSLR [dB]	Az PSLR [dB]	Rg ISLR [dB]	Az ISLR [dB]
X4	SL	34002	0.43 ± 0.03	0.21±0.01	-12.95±0.15	-12.88±0.25	-11.74±0.09	-11.39±0.01
X4	SLH	34056	0.47 ± 0.04	0.21±0.01	-12.97±0.12	-12.82±0.35	-11.68±0.17	-11.42±0.10
X4	SL	34004	0.43 ± 0.03	0.21±0.01	-13.20±0.18	-12.99±0.40	-11.66±0.05	-11.50±0.07
X4	SLH	34054	0.46 ± 0.03	0.23±0.01	-13.05±0.16	-12.83±0.37	-11.67±0.16	-11.38±0.13
X4	SL	36138	0.44 ± 0.03	0.21±0.01	-12.19±0.58	-12.53±0.38	-11.24±0.19	-11.07±0.14
X4	SLH	36139	0.48 ± 0.02	0.22 ± 0.01	-12.57±0.57	-12.47±0.40	-11.87±0.59	-11.16±0.24

Summary of Spatial Resolution Assessment

The overall spatial resolution performance of ICEYE satellite imagery was assessed to be excellent. The spatial resolution in range and azimuth directions of all images was better or in line with the values provided in the ICEYE documentation. From all SM products, slant range resolutions are finer than 1.5 m, and azimuth resolutions are better than 3 m. In addition, from all of SL/SLH products, slant range resolutions are finer than 0.5 m, and azimuth resolutions are within their expected value of 0.25 m.

The measured PSLR and ISLR values are around the expected value provided in the ICEYE documentation. From most images, a PSLR between -12.0 and -13.5 was calculated. Only one SM image and six SL images showed higher than -12.0 dB side lobes, which is approximately 5% of acquisitions in this analysis. Additionally, all the scenes measured better ISLR than the expected value.

1.2 Geolocation Accuracy

4.2.1 Method

The geolocation accuracy was calculated based on the corner reflectors at the calibration sites, a) Rosamond, CA, b) Oklahoma, c) Neustrelitz, Germany, and d) Sodankylä, Finland. The assessment of the ICEYE images was performed using the GAMMA Remote Sensing software and its SLC point target analysis tool, *ptarg_SLC*. An internally developed Python code was used to analyze images with larger than 16-pixel to provide an initial estimation of the CR backscatter. The expected SAR image coordinates of corner reflectors were calculated based on satellite orbit

and their map coordinates and were compared to the SAR image coordinates of the peak signal locations (Figure 11). The geolocation errors were measured in range and azimuth direction separately in absolute values, and the absolute location error (ALE) was then calculated by the equation below:

$$ALE = \sqrt{(Err_{rg,mean})^2 + (Err_{az,mean})^2}$$

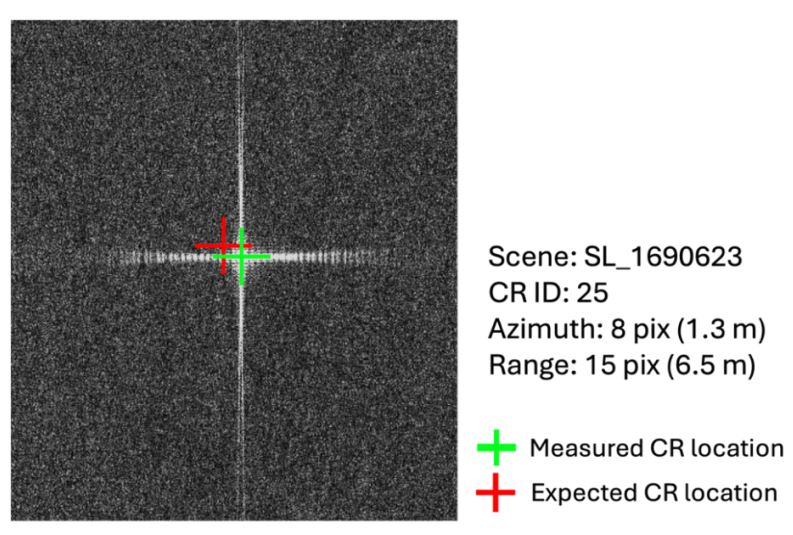


Figure 11. Demonstration of geolocation accuracy assessment. The expected CR location (red) is compared with the observed location in the ICEYE SAR image (green). The image chip is from ICEYE X13 SL_1690623 scene over CR25 at the Rosamond site. The figure shows 8- and 15-pixel offsets in azimuth and range direction between the expected and observed CR location.

4.2.2 Results Compliance

Table 15 shows the quality values related to the geolocation accuracies provided in the ICEYE documentation.

Table 15. Expected geolocation accuracies provided in the ICEYE SAR Product Guide (ICEYE. (2022c).

Image Mode	Geospatial Accuracy [m, CEP90]	3 Sigma (m)
Strip (SM)	6	10.94
Spot (SL, SLH)	6	10.94
Spot Extended Area (SLEA)	6	10.94
Scan (SC)	15	27.35

1.2.1.1 Rosamond, CA, USA

For the Rosamond site, we analysed 29 Strip, 53 Spot, and 4 Scan mode images to calculate geolocation errors. Table 16 lists the results of the geolocation accuracy analysis for the various

ICEYE satellites over the Rosamond site. The table includes the average and the standard deviation of all observed CRs of the scenes. Scenes with larger than expected errors are highlighted in red.

Table 16. Rosamond geolocation accuracy analysis for ICEYE; average and standard deviation of all observed CRs, with larger than expected errors highlighted in red.

Satellite Number	Image Mode	Scene ID	Range Location		Absolute Location
	CM	22720	Error [m]	Error [m]	Error[m]
X2	SM	22728	1.09±0.02	0.53±0.07	1.21
X4	SM	24338	4.65±0.03	2.04±0.05	5.08
X4	SM	29630	3.28±0.03	1.27±0.04	3.52
X4	SM	33818	2.28±0.03	1.36±0.05	2.65
X7	SM	38803	1.89±0.07	422.92±0.07	422.92
X7	SM	41079	11.39±0.03	44.03±0.05	45.48
X2	SM	49376	2.82±0.03	6.11±0.04	6.73
X9	SM	105173	2.65±0.03	1.26±0.09	2.93
X37	SM	950309957	0.10±0.24	1.07±1.44	1.07
X36	SM	950310040	2.41±0.21	0.84±1.10	2.55
X14	SM	950310385	0.54±0.06	4.22±1.36	4.25
X34	SM	950310614	2.43±0.04	6.10±0.07	6.57
X4	SM	20064	2.79±0.02	1.36±0.06	3.10
X5	SM	21756	0.65±0.02	0.83±0.08	1.05
X2	SM	23758	4.34±0.01	4.90±0.06	6.55
X2	SM	33603	2.26±0.02	4.78±0.09	5.29
X2	SM	35082	3.48±0.02	4.41±0.07	5.62
X7	SM	39010	25.61±0.05	664.31±0.10	664.80
X2	SM	39920	3.30±0.02	4.86±0.10	5.87
X2	SM	52027	3.68±0.02	4.53±0.10	5.84
X12	SM	1877717	1.90±0.03	1.95±0.12	2.72
X27	SM	950304863	6.93±0.02	3.40±0.08	7.72
X14	SM	950305095	0.41±0.16	1.28±0.14	1.34
X27	SM	950305577	2.02±0.02	2.65±0.07	3.33
X30	SM	950305792	2.33±0.05	0.12±0.06	2.33
X37	SM	950309860	1.42±0.54	0.39±0.32	1.47
X36	SM	950309942	0.21±0.65	0.27±0.39	0.34
X34	SM	950310092	3.97±0.48	1.23±0.60	4.16
X30	SM	950310551	3.41±0.48	1.19±0.51	3.61
X4	SL	34834	1.74±0.03	1.61±0.04	2.37
X2	SL	35167	2.67±0.03	5.12±0.04	5.77
X4	SL	35640	1.81±0.03	1.29±0.05	2.22
X4	SL	35534	3.78±0.03	2.08±0.05	4.31
X4	SL	36421	13.30±0.03	11.17±0.05	17.37
X4	SL	37413	13.20±0.02	23.29±0.03	26.77
X4	SL	37414	13.69±0.03	19.55±0.04	23.87
X4	SL	38511	1.40±0.03	10.34±0.04	10.43
X4	SL	38600	0.78±0.03	12.96±0.04	12.98
X7	SL	38885	7.74±0.03	294.14±0.06	294.24
X4	SL	40398	1.87±0.03	2.65±0.06	3.24
X4	SL	40525	2.26±0.03	1.34±0.07	2.63
X7	SL	40791	6.41±0.06	1.03±0.04	6.49
X2	SL	40975	2.40±0.03	2.56±0.05	3.51
X7	SL	41078	6.46±0.03	19.76±0.05	20.79
X13	SL	1690623	6.50±0.03	1.35±0.04	6.64

X2	SL	1690628	0.67±0.03	0.04 ± 0.04	0.67
X13	SLH	4018201	0.03 ± 0.02	3.14±0.04	3.14
X7	SLH	4020349	1.36±0.02	0.33 ± 0.07	1.40
X8	SLH	4023256	0.61±0.03	0.46 ± 0.05	0.76
X13	SLH	4024972	1.06±0.03	1.42±0.05	1.77
X7	SLH	4039742	3.32±0.03	2.31±0.04	4.04
X4	SL	32885	2.52±0.03	2.45±0.14	3.51
X4	SL	35590	2.73±0.03	1.87±0.03	3.31
X4	SL	35591	1.01±0.03	1.39±0.06	1.72
X2	SL	36301	4.11±0.03	2.59±0.05	4.86
X4	SL	37327	2.20±0.03	2.20±0.05	3.11
X2	SL	37833	3.58±0.51	3.14±0.35	4.76
X4	SL	38509	2.58±0.53	1.49±0.35	2.98
X4	SL	38510	3.30±0.04	1.04 ± 0.08	3.46
X7	SL	39009	6.56±0.05	3.22±0.04	7.31
X7	SL	39034	26.69±0.52	1212.62±0.36	1212.91
X4	SL	39484	2.24±0.12	1.44±0.33	2.66
X4	SL	40318	1.95±0.09	2.29±0.47	3.01
X4	SL	40393	1.67±0.03	1.32 ± 0.02	2.13
X2	SL	40793	2.27±0.04	2.25±0.14	3.20
X11	SL	1812330	3.75±0.54	6.61 ± 0.38	7.60
X2	SL	1836121	0.76 ± 0.15	7.28 ± 0.43	7.32
X2	SL	1839909	0.70 ± 0.05	6.75±0.10	6.79
X30	SLH	950305104	1.73±0.06	1.54±0.04	2.32
X37	SLH	950305590	0.93±0.05	0.96 ± 0.38	1.34
X36	SLH	950305803	0.73 ± 0.04	1.06 ± 0.03	1.29
X12	SL	1614898	1.71 ± 0.03	0.35 ± 0.03	1.75
X8	SL	1636472	2.66±0.05	1.12±0.10	2.89
X13	SLH	1821032	4.91±0.03	1.42±0.03	5.11
X8	SL	1833902	6.01±0.06	1.19±0.06	6.13
X13	SLH	1835028	3.23±0.03	1.33±0.04	3.49
X11	SL	1703151	1.83±0.04	0.45 ± 0.08	1.88
X11	SL	1790820	1.82±0.03	2.33±0.09	2.96
X8	SL	1827332	0.65±0.25	0.30 ± 0.06	0.72
X13	SLH	1835025	2.18±0.11	2.19±0.09	3.09
X12	SLH	1883416	1.87±0.14	8.47±0.11	8.67
X2	SL	2211313	1.03±0.10	4.82±0.11	4.93
X12	SC	2165262	7.77±2.07	17.58±17.38	19.22
X12	SC	2227690	2.66±7.42	23.52±10.41	23.67
X12	SC	2165261	7.79±6.65	15.94±4.31	17.74
X13	SC	2184970	4.62±4.39	16.56±9.87	17.19

Figures 12 and 13 show plotted azimuth and slant range errors from all SM and SL mode images. In both figures, scenes showing exceptionally high geolocation errors were excluded for the plots. Figure 12 shows that several scenes from the Spot Ascending Left look images, marked as SL_ASC_L, show relatively very large geolocation errors compared to other imaging modes.

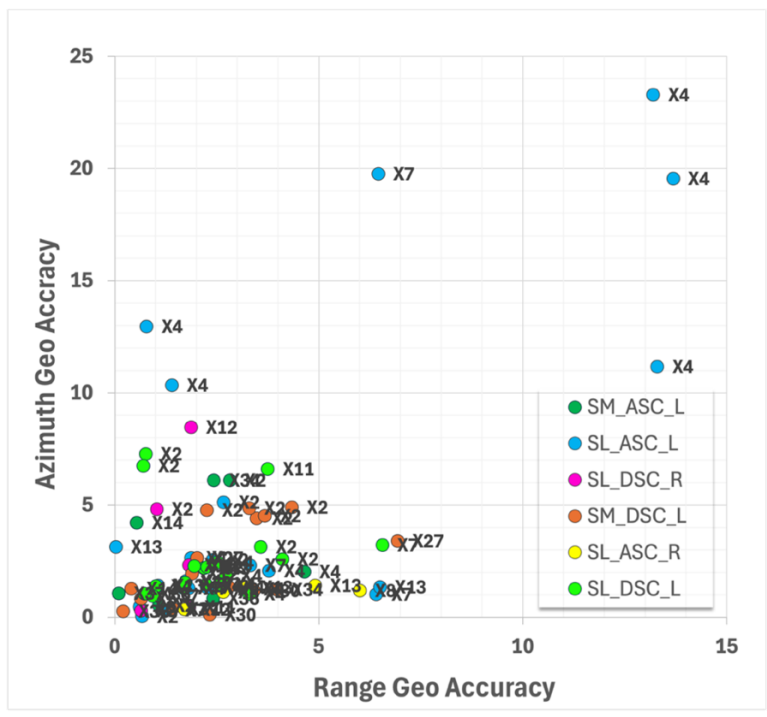


Figure 12. Geolocation errors of all analyzed ICEYE images over Rosamond, CA. Some scenes with larger errors are outside the plotted area. Scenes showing very large geolocation errors were excluded from the plots (ID 38803, 41079, 39010, 38885, 39034).

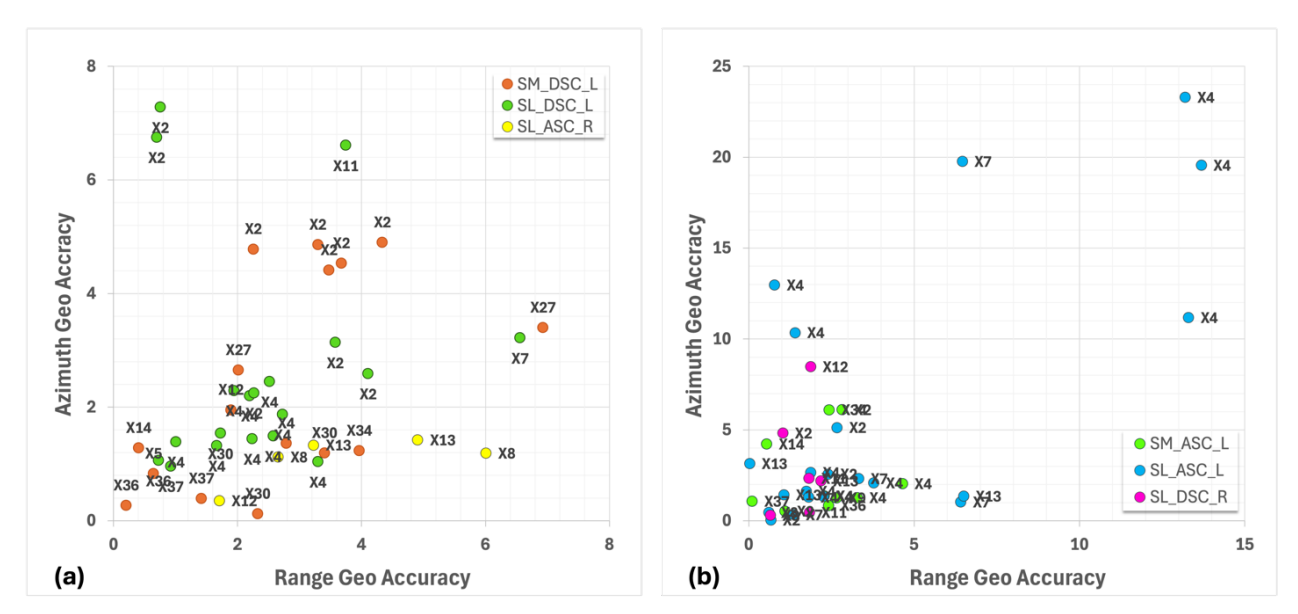


Figure 13. Geolocation errors of ICEYE SM and SL mode images separated according to corner reflector orientation. Each plot shows the mean value of geolocation accuracy of all CRs observed in an image. (a) ICEYE images used for analyzing CRs facing towards west with an azimuth heading of 170°; (b) CRs are oriented mostly towards east with an azimuth heading of 350°. Scenes showing very large geolocation errors were excluded from the plots (ID 38803, 41079, 39010, 38885, 39034).

1.2.1.2 Oklahoma, USA

For the Oklahoma site, we analyzed 19 Strip mode and 7 Spot mode images to calculate geolocation errors. Table 17 presents the results of the geolocation accuracy analysis for various ICEYE satellites over the Oklahoma site, with each scene demonstrating excellent geolocation accuracy.

Table 17. Geolocation accuracy analysis over the Oklahoma site; the values are calculated from a single CR observed within a scene.

Satellite Number	Image Mode	Scene ID	Range Location Error [m]	Azimuth Location Error [m]	Absolute Location Error [m]
X13	SM	4104068	0.26	0.66	0.70
X13	SM	4108639	0.81	0.34	0.88
X13	SM	4113689	0.19	0.46	0.50
X19	SM	4118395	0.42	0.09	0.43
X19	SM	4122012	0.15	0.51	0.53
X20	SM	4103994	0.10	3.31	3.31
X20	SM	4113672	0.21	0.02	0.21
X23	SM	4103993	1.65	0.46	1.71
X31	SM	4102835	2.06	1.56	2.58
X31	SM	4109765	0.85	1.66	1.87
X31	SM	4118393	1.24	4.31	4.48
X35	SM	4108453	3.28	4.13	5.28
X35	SM	4109693	3.91	2.26	4.51
X35	SM	4117243	5.72	1.66	5.96
X7	SM	4107354	0.92	2.28	2.46
X7	SM	4108135	0.55	0.52	0.76
X8	SM	4107633	1.29	2.52	2.83
X8	SM	4122981	0.53	1.33	1.43
X11	SLH	4103169	0.17	2.04	2.05
X11	SLH	4108812	0.36	2.44	2.47
X20	SLH	4109826	2.07	1.16	2.37
X11	SLH	4113700	0.65	1.17	1.34
X11	SLH	4120049	0.30	1.68	1.70
X13	SLH	4123574	0.32	0.16	0.36
X7	SLH	4122664	0.39	1.31	1.37

4.2.2.3 Neustrelitz, Germany

For the Neustrelitz site, we analyzed ten SLH scenes to calculate the geolocation errors. As shown in Table 18, reasonable geolocation errors, consistent with expected values, were observed in both the range and azimuth directions. In addition to the scenes listed in Table 18, we also analyzed the Spot mode image from X12 (scene ID 1883417), which did not appear properly focused. Therefore, geolocation accuracy could not be calculated.

Effective Date: 01/13/2025

Table 18. Geolocation accuracy analysis over the Neustrelitz site; average and standard deviation of all observed CRs.

Satellite Number	Image Mode	Scene ID	Range Location Error [m]	Azimuth Location Error [m]	Absolute Location Error [m]
X13	SLH	1821028	5.38±0.11	0.68±0.33	5.42
X11	SLH	1821033	5.83 ± 0.08	1.02±0.33	5.92
X12	SLH	1839364	4.53±0.07	0.51±0.33	4.56
X13	SLH	1835026	2.68±0.12	2.01±0.32	3.35
X11	SLH	1881654	8.29±0.09	2.38±0.33	8.62
X13	SLH	1876905	8.78 ± 0.07	0.42±0.33	8.79
X11	SLH	1872603	9.91±0.06	6.15±0.33	11.66
X12	SLH	1898700	3.99 ± 0.07	2.31±0.33	4.61
X12	SLH	1923872	1.08±0.15	3.92±0.37	4.07
X12	SLH	1928906	6.03±0.10	1.86±0.32	6.31

4.2.2.4 Sodankylä, Finland

For the Sodankylä site, we analyzed six Spot mode images to calculate geolocation errors. Table 19 presents the results of the geolocation accuracy analysis for the ICEYE X4 satellite over the Sodankylä site, including the average and standard deviation of four CRs in the scenes.

Table 19. Geolocation accuracy analysis over the Sodankylä site; average and standard deviation of all observed CRs.

Satellite Number	Image Mode	Scene ID Range Location Error [m]		Azimuth Location Error [m]	Absolute Location Error [m]
X4	SL	34002	14.30±0.02	1.47±0.22	14.38
X4	SLH	34056	13.10±0.08	2.10±0.10	13.27
X4	SL	34004	11.81±0.10	1.58±0.09	11.92
X4	SLH	34054	14.02±0.06	1.33±0.13	14.08
X4	SL	36138	14.75±0.05	0.63±0.15	14.76
X4	SLH	36139	14.54±0.06	1.05±0.11	14.58

Summary of Geolocation Accuracy Assessment

The overall geolocation performance of ICEYE satellite imagery is assessed to be good. As a result of evaluating geolocation accuracy at the Rosamond site, approximately 88% of the images fell within the expected geolocation error range, although sometimes we found quite large geolocation errors of over 100 m. In addition, the geolocation errors at the Sodankylä site were generally measured to be larger than the stated values in the ICEYE documentation. Only the results from the Oklahoma site showed excellent geolocation accuracy.

Effective Date: 01/13/2025

5. References

- ESA-NASA, (2024). Joint Earth Observation Mission Quality Assessment Framework SAR Guidelines, Rev-002.
- Gelaro, R., McCarty, W., Suárez, M. J., Todling, R., Molod, A., Takacs, L., Randles, C. A., Darmenov, A., Bosilovich, M. G., Reichle, R., & others. (2017). The modern-era retrospective analysis for research and applications, version 2 (MERRA-2). *Journal of Climate*, 30(14), 5419–5454.
- Hooper, A., Segall, P., & Zebker, H. (2007). Persistent scatterer interferometric synthetic aperture radar for crustal deformation analysis, with application to Volcán Alcedo, Galápagos. *Journal of Geophysical Research: Solid Earth*, 112(B7).
- ICEYE. (2020). Level 1 Product Format Specification Document. ICEYE. https://sar.iceye.com/5.1.1/productFormats/metadata/
- ICEYE. (2022a). *ICEYE SAR Data Brochure*. https://iceye.com/hubfs/Downloadables/SAR_Data_Brochure_ICEYE.pdf
- ICEYE. (2022b). *ICEYE SAR Mission Brochure*. https://iceye.com/hubfs/_DATA_AND_MISSIONS/Missions_Brochure_ICEYE.pdf
- ICEYE. (2022c). ICEYE SAR Product Guide. https://sar.iceye.com/5.0/
- Ignatenko, V., Laurila, P., Radius, A., Lamentowski, L., Antropov, O., & Muff, D. (2020). ICEYE Microsatellite SAR Constellation Status Update: Evaluation of first commercial imaging modes. *IGARSS* 2020-2020 *IEEE International Geoscience and Remote Sensing Symposium*, 3581–3584.
- Li, X.-M., & Lehner, S. (2013). Algorithm for sea surface wind retrieval from TerraSAR-X and TanDEM-X data. *IEEE Transactions on Geoscience and Remote Sensing*, 52(5), 2928–2939.
- Marinkovic, P., Ketelaar, G., van Leijen, F., & Hanssen, R. (2007). InSAR quality control: Analysis of five years of corner reflector time series. Proceedings of the Fringe 2007 Workshop (ESA SP-649), Frascati, Italy, 26–30.
- Ruiz, J., & Cohen, J. (2024). *Technical Note on Quality Assessment for ICEYE X11, X12 and X13*. European Space Agency. https://earth.esa.int/eogateway/documents/d/earth-online/technical-note-on-quality-assessment-for-iceye-x11-x12-x13
- Ulaby, F., Dobson, M. C., & Álvarez-Pérez, J. L. (2019). *Handbook of radar scattering statistics for terrain*. Artech House.

Rev- 001

Effective Date: 01/13/2025

Van Zyl, J. J. (1990). Calibration of polarimetric radar images using only image parameters and trihedral corner reflector responses. *IEEE Transactions on Geoscience and Remote Sensing*,

28(3), 337–348.

Rev- 001

APPENDIX A

Table A1. Detailed list of ICEYE acquisitions used for the radiometric assessment.

Test Area	Satellite Number	Imaging Mode	Scene ID	Acquisition Date	Incidence Angle	Processor Version
Rosamond, CA	Х9	SM	105173	20210816	29.4	1.916
	X2	SM	22728	20200222	32.9	1.916
	X4	SM	24338	20200318	30.8	1.916
	X4	SM	29630	20200527	28.4	1.916
	X4	SM	33818	20200805	33.3	1.916
	X7	SM	38803	20201211	28.9	1.916
	X7	SM	41079	20210130	33.7	1.916
	X2	SM	49376	20210325	28.6	1.916
Rosamond, CA	X7	SM	582083	20220510	36.8	1.94
(GTR)	X7	SM	582085	20220511	36.9	1.94
	X7	SM	593227	20220519	36.8	1.94
	X7	SM	593228	20220520	36.7	1.94
	X7	SM	593229	20220521	36.8	1.94
	X7	SM	593230	20220522	36.7	1.94
	X7	SM	609280	20220523	36.6	1.94
	X7	SM	609281	20220524	36.6	1.94
	X7	SM	609282	20220525	36.6	1.94
	X7	SM	609283	20220526	36.5	1.94
	X7	SM	609284	20220527	36.5	1.94
	X7	SM	630348	20220531	36.5	1.94
	X7	SM	630349	20220601	36.5	1.94
	X7	SM	630350	20220602	36.5	1.94
	X7	SM	638181	20220603	36.4	1.94
	X7	SM	647284	20220609	36.4	1.94
	X7	SM	650383	20220608	36.4	1.94
	X7	SM	685382	20220611	36.3	1.94
	X7	SM	808334	20220719	36.1	1.94
	X7	SM	808335	20220720	36.2	1.94
	X7	SM	810542	20220717	36.1	1.94
	X7	SM	909101	20220810	36.7	1.94
	X7	SM	909103	20220812	36.8	1.94
	X7	SM	909105	20220818	36.8	1.94
	X7	SM	909106	20220819	36.8	1.94
	X7	SM	909108	20220821	36.7	1.94
	X7	SM	928357	20220826	36.9	1.94
	X7	SM	933715	20220827	37.0	1.94
	X7	SM	947330	20220828	37.0	1.94
	X7	SM	1082003	20220829	37.1	1.94
	X7	SM	1117559	20220905	37.1	1.94
Doldrums	X13	SLEA	2051939	20230407	20.9	1.1
	X8	SLEA	2051943	20230408	23.1	1.1
	X8	SLEA	2051951	20230408	22.4	1.1
	X11	SLEA	2051958	20230408	24.5	1.1
	X2	SLEA	2051944	20230408	26.7	1.1
	X12	SLEA	2051948	20230408	23.1	1.1
	X11	SLEA	2051949	20230408	29	1.1

Test Area	Satellite Number	Imaging Mode	Scene ID	Acquisition Date	Incidence Angle	Processor Version
	X13	SLH	1801605	20230120	29.7	1.1
	X11	SLH	1801594	20230120	29.6	1.1
	X12	SLH	1801600	20230121	29.7	1.1
	X11	SLH	1801595	20230121	29.6	1.1
	X11	SLH	1801597	20230122	29.5	1.1
	X13	SLH	1801607	20230122	29.7	1.1
	X27	SLH	950305096	20240531	26.2	1.916
	X27	SLH	950305224	20240601	39.3	1.916
	X14	SLH	950305349	20240602	26	1.916
	X34	SLH	950305424	20240603	39.1	1.916
	X20	SLH	4139872	20240630	23.6	1.101
	X7	SM	4103194	20240530	29.5	1.1
	X27	SM	950304725	20240530	23.5	1.916
	X8	SM	4106576	20240601	14	1.1
	X31	SM	4107635	20240602	17.9	1.1
	X37	SM	950305430	20240603	32.7	1.916
	X27	SM	950305539	20240604	22.1	1.916
Amazon	X11	SC	4140890	20240701	23.2	1.101
	X35	SC	4141133	20240701	23.6	1.101
	X37	SLEA	950305184	20240601	32.4	1.916
	X14	SLEA	950305784	20240605	32.9	1.916
	X31	SLEA	4140357	20240630	20.5	1.101
	X11	SLEA	4141849	20240702	35.1	1.101
	X7	SLH	58351	20210529	20.9	1.1
	X7	SLH	58353	20210530	30.5	1.1
	X7	SLH	58354	20210531	30.6	1.1
	X13	SLH	1801226	20230126	21	1.1
	X11	SLH	1803337	20230129	32.5	1.1
	X13	SLH	1813154	20230129	31.1	1.1
	X12	SLH	1817734	20230201	32.5	1.1
	X12	SLH	1835808	20230203	21.2	1.1
	X12	SLH	2205700	20230531	22.4	1.1
	X12	SLH	2205701	20230601	25.3	1.1
	X8	SLH	2205702	20230602	20.8	1.1
	X13	SLH	2214797	20230603	24.3	1.1
	X14	SLH	950304788	20240530	29.4	1.916
	X34	SLH	950305085	20240531	31	1.916
	X27	SLH	950305413	20240603	25.5	1.916
	X34	SLH	950305787	20240605	30.6	1.916
	X34	SLH	950306958	20240610	32.7	1.916
	X20	SLH	4137353	20240628	34.3	1.101
	X31	SLH	4137219	20240628	29.6	1.101
	X13	SLH	4140894	20240701	26.4	1.101
	X34	SM	950304860	20240530	27.9	1.916
	X30	SM	950305183	20240601	16	1.916
	X27	SM	950305112	20240601	15.8	1.916
	X17	SM	950305346	20240602	27.1	1.916
	X37	SM	950305418	20240603	22.2	1.916
	X36	SM	950305524	20240604 20240604	28.6	1.916
	X34	SM SM	950305561		27.6	1.916
	X13	SM	4114198	20240608	24.3	1.1

Satellite **Imaging** Acquisition Incidence Processor **Test Area Scene ID** Version Number Mode Angle Date 20240608 26.7 X8 SM 4114267 1.1 X14 SM 950308320 20240618 33.3 1.916

Table A2. Detailed list of ICEYE acquisitions used for the IRF assessment.

Test Area	Satellite Number	Imaging Mode	Scene ID	Acquisition Date	Incidence Angle	Processor Version
Rosamond,	X2	SM	22728	20200222	32.9475	1.916
California	X4	SM	24338	20200318	30.8634	1.916
	X4	SM	29630	20200527	28.5053	1.916
	X4	SM	33818	20200805	33.3925	1.916
	X7	SM	38803	20201211	29.0052	1.916
	X7	SM	41079	20210130	33.7990	1.916
	X2	SM	49376	20210325	28.6541	1.916
	X9	SM	105173	20210816	29.4459	1.916
	X37	SM	950309957	20240701	28.8860	1.101
	X36	SM	950310040	20240702	26.0901	1.101
	X14	SM	950310385	20240708	21.2453	1.101
	X34	SM	950310614	20240711	27.3458	1.101
	X4	SM	20064	20200131	31.8588	1.916
	X5	SM	21756	20200220	30.6302	1.916
	X2	SM	23758	20200309	29.0092	1.916
	X2	SM	33603	20200731	27.4640	1.916
	X2	SM	35082	20200905	27.8326	1.916
	X7	SM	39010	20201216	30.1259	1.916
	X2	SM	39920	20210109	27.2273	1.916
	X2	SM	52027	20210410	28.3101	1.916
	X12	SM	1877717	20230214	26.6283	1.916
	X27	SM	950304863	20240530	31.3716	1.916
	X14	SM	950305095	20240531	35.0269	1.916
	X27	SM	950305577	20240604	30.3204	1.916
	X30	SM	950305792	20240605	34.8003	1.916
	X37	SM	950309860	20240629	22.5229	1.916
	X36	SM	950309942	20240630	26.4467	1.916
	X34	SM	950310092	20240702	16.4963	1.101
	X30	SM	950310551	20240710	16.4963	1.101
	X4	SL	34834	20200830	20.7382	1.1
	X2	SL	35167	20200907	30.1627	1.1
	X4	SL	35640	20200921	34.2906	1.1
	X4	SL	35534	20200922	27.0033	1.1

Test Area	Satellite Number	Imaging Mode	Scene ID	Acquisition Date	Incidence Angle	Processor Version
	X4	SL	36421	20201015	33.8482	1.1
	X4	SL	37413	20201108	34.1643	1.1
	X4	SL	37414	20201109	26.6161	1.1
	X4	SL	38511	20201202	34.5847	1.1
	X4	SL	38600	20201203	27.2991	1.1
	X7	SL	38885	20201212	31.8041	1.1
	X4	SL	40398	20210120	33.2695	1.1
	X4	SL	40525	20210121	26.0451	1.1
	X7	SL	40791	20210127	21.1803	1.1
	X2	SL	40975	20210129	32.0711	1.1
	X7	SL	41078	20210129	29.2924	1.1
	X13	SL	1690623	20221228	30.9828	1.916
	X2	SL	1690628	20230103	31.6774	1.916
	X13	SLH	4018201	20240404	29.8292	1.1
	X7	SLH	4020349	20240407	24.4133	1.1
	X8	SLH	4023256	20240411	29.8182	1.1
	X13	SLH	4024972	20240413	20.8492	1.1
	X7	SLH	4039742	20240423	31.9319	1.1
	X4	SL	32885	20200711	26.5352	1.1
	X4	SL	35590	20200920	27.2908	1.1
	X4	SL	35591	20200921	34.7377	1.1
	X2	SL	36301	20201011	28.3940	1.1
	X4	SL	37327	20201107	28.1152	1.1
	X2	SL	37833	20201116	27.2762	1.1
	X4	SL	38509	20201201	26.9627	1.1
	X4	SL	38510	20201202	34.1238	1.1
	X7	SL	39009	20201215	33.9869	1.1
	X7	SL	39034	20201217	26.7101	1.1
	X4	SL	39484	20201225	24.8889	1.1
	X4	SL	40318	20210118	21.0361	1.1
	X4	SL	40393	20210119	21.0361	1.1
	X2	SL	40793	20210127	29.0577	1.1
	X11	SL	1812330	20230122	26.8050	1.1
	X2	SL	1836121	20230130	27.3133	1.916
	X2	SL	1839909	20230131	21.4935	1.1
	X30	SLH	950305104	20240531	27.4729	1.916
	X37	SLH	950305590	20240604	37.2182	1.916
	X36	SLH	950305803	20240605	27.7085	1.916
	X12	SL	1614898	20221213	28.4389	1.1

Test Area	Satellite Number	Imaging Mode	Scene ID	Acquisition Date	Incidence Angle	Processor Version
	X8	SL	1636472	20221216	26.5588	1.1
	X13	SLH	1821032	20230128	26.9577	1.1
	X8	SL	1833902	20230130	31.2773	1.1
	X13	SLH	1835028	20230205	23.9442	1.1
	X11	SL	1703151	20230101	28.5840	1.1
	X11	SL	1790820	20230118	35.4778	1.1
	X8	SL	1827332	20230127	22.8707	1.1
	X13	SLH	1835025	20230201	21.8219	1.1
	X12	SLH	1883416	20230216	31.5399	1.1
	X2	SL	2211313	20230601	33.5557	1.1
	X12	SC	2165262	20230522	24.1596	1.916
	X12	SC	2227690	20230616	29.4648	1.916
	X12	SC	2165261	20230516	29.5819	1.916
	X13	SC	2184970	20230531	21.4994	1.916
Oklahoma,	X13	SM	4104068	20240530	15.7514	1.1
USA	X13	SM	4108639	20240603	34.6509	1.1
	X13	SM	4113689	20240607	33.808	1.1
	X19	SM	4118395	20240611	21.752	1.1
	X19	SM	4122012	20240614	26.4992	1.1
	X20	SM	4103994	20240530	16.1614	1.1
	X20	SM	4113672	20240607	20.7404	1.1
	X23	SM	4103993	20240530	22.8957	1.1
	X31	SM	4102835	20240529	18.9025	1.1
	X31	SM	4109765	20240604	27.4114	1.1
	X31	SM	4118393	20240611	29.7755	1.1
	X35	SM	4108453	20240603	34.2435	1.1
	X35	SM	4109693	20240604	19.2358	1.1
	X35	SM	4117243	20240610	24.6754	1.1
	X7	SM	4107354	20240602	28.8528	1.1
	X7	SM	4108135	20240603	28.8773	1.1
	X8	SM	4103746	20240530	18.0604	1.1
	X8	SM	4107633	20240602	31.1776	1.1
	X8	SM	4122981	20240615	17.598	1.1
	X11	SLH	4103169	20240529	31.677	1.1
	X11	SLH	4108812	20240603	23.9228	1.1
	X20	SLH	4109826	20240604	37.8026	1.1
	X11	SLH	4113700	20240607	35.1299	1.1
	X11	SLH	4120049	20240612	24.5534	1.1
	X13	SLH	4123574	20240615	36.9466	1.1

Test Area	Satellite Number	Imaging Mode	Scene ID	Acquisition Date	Incidence Angle	Processor Version
	X7	SLH	4122664	20240615	26.0671	1.1
Neustrelitz,	X13	SLH	1821028	20230126	23.3703	1.1
Germany	X11	SLH	1821033	20230130	28.1896	1.1
	X12	SLH	1839364	20230201	29.5324	1.1
	X13	SLH	1835026	20230203	21.8082	1.1
	X11	SLH	1881654	20230215	26.3632	1.1
	X12	SLH	1883417	20230217	33.3238	1.1
	X13	SLH	1876905	20230218	29.4445	1.1
	X11	SLH	1872603	20230220	31.4961	1.1
	X12	SLH	1898700	20230225	30.7164	1.1
	X12	SLH	1923872	20230303	29.8399	1.1
	X12	SLH	1928906	20230305	24.6927	1.1
Sodankylä,	X4	SL	34002	20200823	26.3688	1.1
Finland	X4	SLH	34056	20200915	23.791	1.1
	X4	SL	34004	20200916	27.476	1.1
	X4	SLH	34054	20201008	21.3028	1.1
	X4	SL	36138	20201101	21.8349	1.1
	X4	SLH	36139	20201102	25.6782	1.1